

# **Defining Binding Principles to Target the Coactivator Med25-Activator Interaction**

by

Nicholas J. Foster

A dissertation submitted in partial fulfillment  
of the requirements for the degree of  
Doctor of Philosophy  
(Chemical Biology)  
in the University of Michigan  
2021

Doctoral Committee:

Professor Anna Mapp, Chair  
Assistant Professor Amanda Garner  
Associate Professor Jolanta Grembecka  
Professor John Montgomery

Nicholas J. Foster

fosten@umich.edu

ORCID iD: 0000-0002-1034-6596

© Nicholas J. Foster

## **Acknowledgements**

First, I would like to thank Dr. Cherie Dotson. My serious thoughts of graduate school began while attending the Interdisciplinary Research Experience for Undergraduates (IREU) which she organizes through the College of Pharmacy. During that time, I was able to meet a group of great people who were also emerging scientists. Glad to still hear from some of them. One of the major highlights of that experience was being able to meet Dr. Evans. I was really surprised to talk to a scientist that knew the location my hometown and a lot about it.

I'd also like to thank my research advisor Dr. Anna Mapp. While participating in the IREU summer program in 2014, I worked in her lab and began learning how to formulate questions and apply appropriate techniques to conduct sound, scientific experiments. I later joined Michigan and her lab. Thanks for your patience during my time working in your lab. Thanks for allowing me to join.

I would also like to recognize my committee members - Professors Amanda Garner, John Montgomery, and Jolanta Grembecka. The recommendations and advice given by way of committee meetings helped me to grow academically and think outside of the box as a chemical biologist.

Next, recognition is in order to my lab members. My lab members are a fun group to be around. It was exciting hearing the stories told most days in lab. Thanks also for

being helpful resources when projects didn't go as planned as well. Much success to you all.

Lastly, I'd like to thank my family. My family is a very important part of me. Thanks to my parents and older brother for being a great support system while making it to this milestone. My father who was a diligent and hardworking man always kept me inspired. His consistency is something I always looked at as an example to pattern myself after. Rest easy pop, love you always. My mother is loving and supportive and keeps me grounded. She encourages me to never count myself out. I appreciate the things you do. I want to acknowledge my older brother. He always pushes me to do bigger and better things constantly. My family was very instrumental in giving me encouraging words during difficult points while working towards this goal. Also thanks to my friends and neighbors back home as well that always keep in contact and have uplifting conversations with me. My hope is that this will serve as an example to young ones from my neighborhood and hometown to show there are other ways to progress yourself outside of being an athlete or some sort of entertainer. GO BLUE !

## Table of Contents

Acknowledgements	ii
List of Figures	vii
List of Tables	ix
List of Abbreviations	x
List of Appendices	xi
Abstract	xii
<b>Chapter 1. Targeting Therapeutically Relevant Mediator Tail Subunits</b>	
1.1 Abstract	1
1.2 The Components and Function of the Pre-Initiation Complex	1
1.3 The Mediator Complex	4
1.4 The Med25 Subunit	7
1.5 The Challenge of Drugging Protein-Protein Interactions	9
1.6 Thesis Summary	15
1.7 References	16
<b>Chapter 2. Interrogating Coactivator Med25-Activator Interaction</b>	
2.1 Abstract	22
2.2 Introduction	23
Mediator Complex Subunit Med25	23

2.3 Results and Discussion	27
Dissection of Activator Binding Location	27
The Role of Electrostatics in Activator Interactions with Med25-AcID	29
2.4 Conclusions	35
2.5 Materials and Methods	37
Plasmids	37
Protein Expression and Purification	38
Peptide Synthesis	38
Direct Binding Experiments	40
Modeling Experimental	41
2.6 References	42
<b>Chapter 3. Using Covalent Fragment to Target a Key Dynamic Substructure in Med25</b>	
3.1 Abstract	47
3.2 Introduction	47
Covalently Targeting Dynamic Proteins	47
3.3 Results and Discussion	51
Fragment Discovery in Med25 Using Disulfide Tethering	51
Targeted Dynamic Substructure Allows for Allosteric Modulation	56
3.4 Conclusions	59
3.5 Materials and Methods	60
3.6 Reference	62

## **Chapter 4. Conclusions and Future Directions**

4.1 Conclusions of this work	66
4.2 Future Directions	70
Electrostatic Selectivity	71
Further Disulfide Fragment Assessment	71
4.3 References	73

## List of Figures

Figure 1.1 The Pre-Initiation Complex	2
Figure 1.2 Structure of Mediator reported in literature	5
Figure 1.3 The surface area-affinity relationship	10
Figure 1.4 Techniques used for small molecule discovery for dynamic proteins	12
Figure 2.1 The Mediator's Subunit Med25	24
Figure 2.2 Erm and ATF6 $\alpha$ bind opposite surfaces in NMR studies	28
Figure 2.3 Mutagenesis shows ATF6 $\alpha$ engages the H2 binding surface	29
Figure 2.4 Positive Residues of AcID & Negative Residues of Binding Activators	30
Figure 2.5 The Hofmeister Series	31
Figure 2.6 Salt anions change activator affinity	32
Figure 2.7 Salt cation size changes activator affinity	33
Figure 2.8. Erm soft mutations alter affinity	34
Figure 2.9 Med25-Activator interaction binding model	37
Figure 3.1 Tethering Schematic	48
Figure 3.2 Disulfide Fragment Targets KIX dynamic structure	49
Figure 3.3 Cartoon representation of Med25-AcID with the domain's native cysteine residues shown in red spheres	50



Figure 3.4 Med25-AcID native cysteine accessibility	51
Figure 3.5 Results of the tethering screen with wild-type Med25-AcID and C506C mutant	54
Figure 3.6 Fragment 22 alters activator binding to Med25	56
Figure 3.7 Tethering efficiency of fragment 22 derivatives	57
Figure 3.8 Signs of Med25-AcID stabilization from fragment 22	59

## List of Tables

Table 1.1 Mediator's Activator Binding Tail Subunits	7
Table 1.2 Activation mechanism and associated phenotypes of listed ETV transcription factor members	9
Table 1.3 Coactivator Protein Inhibitors	13
Table 2.1 The Net Charge of Activator Binding Proteins	26
Table 3.1 The Mass Spectrometry Tethering Screen Results	52

## List of Abbreviations

ATF6 $\alpha$	Activation transcription factor 6 $\alpha$
CBP	CREB binding protein
DNA	Deoxyribonucleic acid
DSF	Differential Scanning Fluorimetry
Ets	E-twenty six
ETV	Ets translocation variant
GTF	General transcription factor
Hif1 $\alpha$	Hypoxia inducible factor 1 $\alpha$
KIX	Kinase inducible domain interaction domain
Med25	Mediator subunit 25
MLL	Mixed Lineage Leukemia
MMP-2	Matrix Metalloprotease-2
NR	Nuclear Receptor
PPI	Protein-protein interaction
RNA	Ribonucleic acid
VP16	Herpes simplex virus protein 16
VWA	Von Williebrand Factor Type A

## List of Appendices

Appendix A. Characterization of Synthesized Peptides	77
Appendix B. NMR Chemical Shift Perturbations	80

## Abstract

Transcription is the process by which the information encoded in our DNA is converted to RNA. This important event is guided by an assembly of proteins brought together at specific gene promoter sites. A key part of the assembly is a coactivator complex called Mediator that interacts with transcriptional activator proteins. Mediator is therapeutically relevant because these interactions are misregulated in many diseases. Unfortunately, the coactivator class of proteins are notoriously difficult to target with druglike molecules. Coactivators are usually dynamic in nature and poorly understood mechanistically, making it quite challenging to design or discover small molecule modulators. Because of this, there is a lack of useful small molecule probes that target coactivators such as those within the Mediator complex.

The coactivator Med25 is a component of Mediator that binds transcriptional activators using its Activator Interaction Domain (AcID) and there is considerable evidence that its network of protein-protein interactions (PPIs) are dysregulated in certain cancers. Although Med25 is conformationally dynamic like other coactivators, Med25-AcID has a structurally unique fold. It contains a central  $\beta$ -barrel that is flanked by dynamic loop and helix substructures and the prevailing structural model is that the featureless surfaces of the  $\beta$ -barrel are the key binding surfaces for activators. This dissertation defines important binding mechanism principles for Med25-AcID and activator protein interactions that allow for small molecule probes. It was found using a series of binding

and mutagenesis structures that the activators ATF6 $\alpha$  and ERM, despite sequence similarities, bind to opposite faces of the AcID  $\beta$ -barrel. Further computational and binding experiments revealed that charge-containing dynamic loop structures adjacent to the binding surfaces are important in these interactions.

In Chapter 3, I report the successful targeting of one of the dynamic substructures in Med25 with a covalent disulfide fragment that influences the conformation and binding of Med25-AcID. This was accomplished through a mass spectrometry based Tethering screen used because of our lab's previous success in targeting dynamic coactivator proteins. A disulfide fragment library was used to identify a lead fragment that changes the kinetic  $k_{\text{off}}$  signature of two Med25-binding activators. Furthermore, the fragment stabilizes the AcID domain and uses a chiral surface that allows for sufficient disulfide exchange that may prove beneficial in changing activator binding effects. Taken together, results defined in this thesis will provide a framework to learning about coactivator-activator interaction's mechanistic features to discover probes for this class of proteins.

## **Chapter 1.**

### **Targeting Therapeutically Relevant Mediator Tail Subunits**

#### **1.1 Abstract**

Transcription is the process whereby DNA is converted into RNA and is thus a critical step in gene expression. One important component of this process is the pre-initiation complex (PIC), a multi-protein complex that forms proximal to a gene just before the start of transcription. The assembly and function of the complex relies on a number of protein-protein interactions (PPIs) that are valuable therapeutic targets due to their connections with disease. For example, misregulation of the PPIs formed between the Mediator complex's tail module and transcription factors such as ETV1 and ERM are implicated in oncogenesis and metastasis in breast and prostate cancer. However, there have been challenges that have hampered drug discovery targeting transcriptional PPIs. In Chapter 1, we outline the general working components of the PIC that help accomplish transcription, with a particular focus on Mediator and its constituent coactivator proteins. The importance of individual protein-protein interactions and their biophysical characteristics are also discussed. Lastly, commonly used strategies in targeting protein-protein interactions are highlighted.

#### **1.2 The Components and Function of the Pre-Initiation Complex**

Formation of the pre-initiation complex (PIC) is a key step in eukaryotic transcription, as it recruits and orients RNA polymerase II at the transcriptional start site. The minimal components of the pre-initiation complex include the general transcription factors (GTFs) TFIIA, TFIIB, TFIID, TFIIE, TFIIF, and TFIIH; the Mediator coactivator complex; and RNA polymerase II.<sup>20</sup> The GTFs were first identified through fractionation of nuclear extracts to elucidate factors that allowed RNA polymerase II to transcribe DNA. Assembling in a step-wise fashion, the GTFs orient the PIC and the polymerase (TFIID) as well as unwind and melt the DNA (TFIIH). It was subsequently found that a fully functional PIC also requires the Mediator complex, a transcriptional coactivator that forms protein-protein interaction (PPI) networks with transcriptional factors (Figure 1.1).

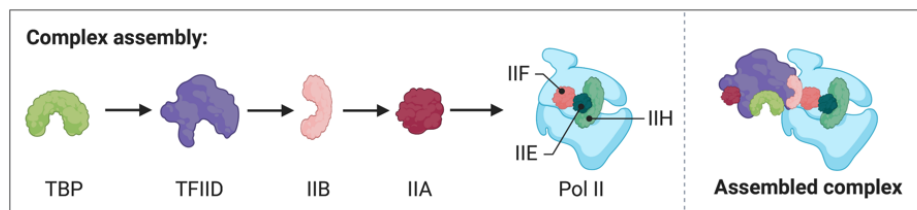
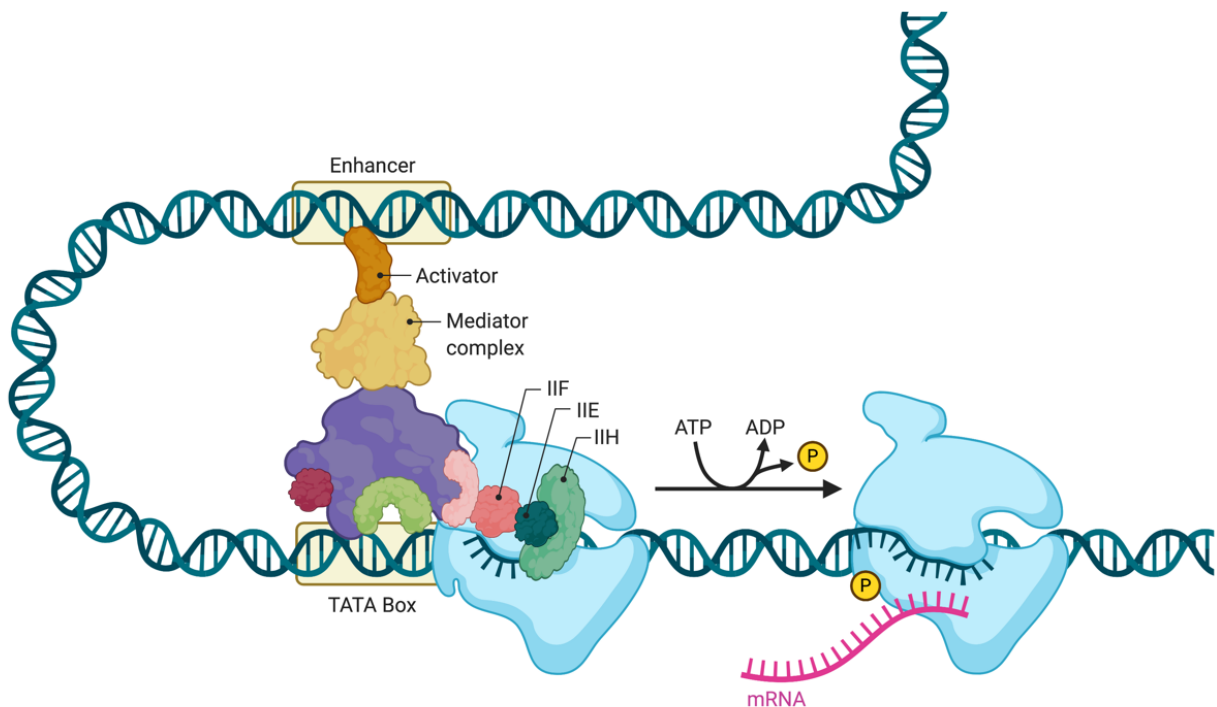




**Figure 1.1** The Pre-Initiation Complex. Components of the pre-initiation complex such as GTFs, coactivator complexes, and transcription factors are recruited to DNA help start gene transcription. Figure created in Biorender.com.

The protein-protein interactions underpinning PIC formation are strictly regulated due to their fundamental role in gene expression. Post-translational modifications, subcellular localization changes, and phase separations all regulate the timing and location of PIC assembly. Dysregulation of the PPI network is thus associated with human diseases, from cancer to developmental disorders. For example, mutations in the TFIIH subunits p8 and p52<sup>10</sup> alter interactions within the complex and are correlated with developmental disorders. In the case of TFIIIB, mutations in the TBP subunit lead to spinocerebellar ataxia and in Taf1 are linked to intellectual disabilities.<sup>12</sup> Despite these connections with disease, the GTFs are not good targets for therapeutic discovery because they are required for transcription of nearly all class II genes.<sup>23</sup>

As noted above, Mediator is a coactivator complex involved in the pre-initiation complex. This complex plays an important role with regard to the architecture of the pre-initiation complex, as it forms a bridge between DNA-bound transcription factors and RNA polymerase II. More recent structural and functional data have revealed that individual subunits of Mediator (subunits 20-25) play roles beyond the architectural, however.<sup>26</sup> The protein subunits that bind to transcription factors are of most interest from a drug discovery standpoint. Their transcription factor PPI networks are frequently dysregulated in disease and, as elaborated in the next section, the subunits are not required for general transcription.

### 1.3 The Mediator Complex

As a part of the pre-initiation complex, Mediator is involved in RNA polymerase II transcription. Before discovery of the Mediator complex, it was thought that the general transcription factors (TFIIA, IIB, IID, IIE, IIF, and IIH) along with polymerase II represented a complete transcription system.<sup>14</sup> However, later work by Dr. Roger Kornberg identified the Mediator complex in yeast that appeared to interact directly with DNA-bound transcription factors. Early evidence of Mediator stemmed from squelching experiments. Squelching referred to the idea that overexpression of one activator affected the function of others due to activators competing for a common target. Kornberg and colleagues found that a crude fraction isolated from yeast was able to relieve squelching induced by the Gal4+VP16 activator and further fractionation revealed that the relevant component was Mediator.<sup>13</sup> Decades of subsequent work led to the identification of 25 individual components of yeast Mediator while mammalian Mediator contains 33 subunits. There have been differences in the reported number of subunits that are present in the Mediator in literature.<sup>6</sup> This complex transfers information from DNA-bound transcription factors to the GTFs and polymerase II assembly through protein-protein interactions. It has roles in polymerase II C-terminal domain (CTD) phosphorylation as well.

Structurally, Mediator is divided into the head, middle, tail, and kinase modules, where the Med14 subunit stabilizes its assembly (Figure 1.2). El Khattabi et al. report cryo-EM studies of mammalian Mediator at 5.9 Å. The head and middle modules in the 5.9 Å structure were identified based upon homology to the *S. pombe* Mediators, while some of the tail module was identified through deletion and mass spectrometry-based cross-linking methods.

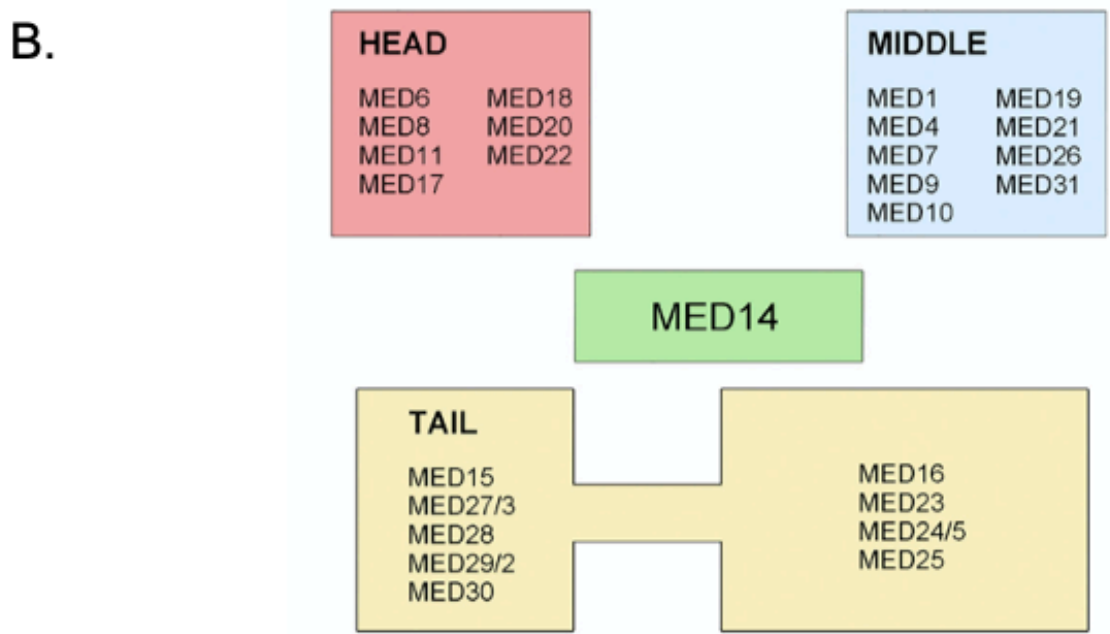
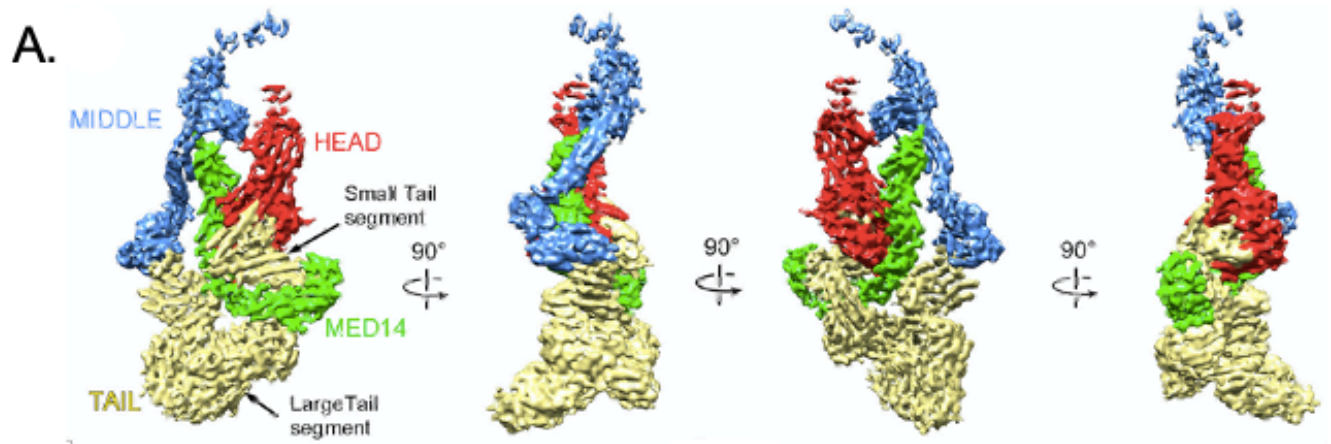


**Figure 1.2** Structure of Mediator reported in literature. (A) shows the head (Red), Middle (Blue), and Tail (Yellow) reported at angles rotated at 90° angles. (B) The subunits are compartmentalized by sections of the Mediator. This figure was used with the permission of publisher.

The Mediator complex has an important role in the architecture of the PIC by bridging transcription factors to the general components required for basal level transcription.

Outside of this, it has other functions. RNA-Sequencing (RNA-Seq) studies of Mediator-depleted cells show there is a ~7-fold downregulation of the transcriptome.<sup>9</sup> The head and middle modules, which is considered the “core Mediator”, interacts with RNA polymerase II and are critical for regulated transcription. The tail module has exchangeable subunits that can vary depending on context.

The tail module is segmented into two connected sections. One comprises the upper portion, which is smaller in size and closest to the head module which is more architectural module. The second is the larger that is ~380 kDa in size. Experiments with knockout tail subunits showed slight changes to polymerase II activity while, the opposite effect was seen with head and middle module knockout experiments. There are specific subunits in the larger tail module like Med15, Med 23, and Med25 that are known to interact with transcription factors and especially transcriptional activators. For example, yeast Med15 is known to bind to Gal4, Gcn4<sup>5</sup>, and VP16 activators.<sup>29</sup> The Arc105/Med15 subunit in humans complexes with SREBP transcription factors and in doing so regulates lipid homeostasis.<sup>35</sup> And, as outlined in more detail in the subsequent section, Med25 forms PPIs with the ETV/PEA family of ETS transcription factors as well as the stress-response transcription factor ATF6 $\alpha$ .<sup>32,25,15,3</sup> The coactivator subunits of the tail are also known to be associated with a number of diseases. Subunits such as Med23 are good examples. Loss of the metastasis suppressor gene KiSS-1 is heavily involved in cancer.<sup>22</sup> Studies have shown KiSS-1 gene expression in metastasis is regulated through specificity protein-1 and its interaction with Med23. Other components of the tail module are exchangeable as reported in biochemical data.

**Table 1.1 Mediator's Activator Binding Tail subunits**

<b>Activator-Binding Tail Subunits</b>	<b>Activators</b>
Med15/Arc105	GCN4, Pho4, Msn2 <sup>24</sup> , Ino2, VP16, Pdr1, SREBP
Med23	Elk1 <sup>27</sup> , Elf3 <sup>2</sup> , Sp1
Med25	VP16, Erm, ETV1, ETV4, ATF6 $\alpha$ , p53 <sup>17</sup> , cJun

**1.4 The Med25 subunit**

The Med25 subunit of the tail module contains at least three protein-protein interaction domains. They are the von Willebrand factor A (VWA), activator interaction domain (AcID), and nuclear receptor box (NR). The VWA domain binds the rest of Mediator complex, and AcID interacts with activation regions of transcription factors. The last domain is located in the C-terminal region and binds nuclear receptors. Med25 has been shown to regulate drug and lipid metabolism through HNF4 $\alpha$  genes, where HNF4 $\alpha$  is in the class of orphan nuclear receptors.

As shown above, Med25 has domains designated for interacting with different partners. The Med25-AcID and transcription factor binding event is preferred because the activation domain of transcription factors allow for studying a particular set of therapeutically relevant genes outside of the GTF's large range of genes. Med25-AcID alone binds many different transcription factors. It is able to bind the ETV family transcription factors. The subfamilies ETV1, 4, and 5 bind with an affinity of ~500 nM. These activators use a 30-residue binding region (the transcriptional activation domain).<sup>7</sup>

Overexpression of the Med25-AcID or the VWA domain inhibits ETV-mediated transcription of reporter genes in a range of promoter contexts (Table 1.2). It also interacts with the herpes simplex virion protein 16 (VP16). VP16 controls the transcription of immediate early viral genes.<sup>33,28</sup> Other transcription factors such as ATF6 $\alpha$  binds as well, and it is involved in endoplasmic reticulum stress response.

Med25-AcID is considered a hub motif because it can bind a variety of different binding partners using two conserved binding surfaces. In addition, there is also no crystal structure available due to its' dynamic characteristics. Early NMR structural work carried out, showed Med25-AcID has a  $\beta$ -barrel framed by flexible substructures. Questions immediately rose pertaining to its binding mechanism seeing its drastically different to other better studied coactivators such as CBP KIX. Learning about Med25-AcID binding mechanism will help guide small molecule discovery seeing there has been lacking information. It will also allow us to extract guiding principles that can then be compared to common coactivator transcription factor interacting networks. Lastly, it allows us to make connections between structure-function relationships in the context of different affiliated diseases.<sup>31</sup>

**Table 1.2** Activation mechanism and associated phenotypes of listed ETV transcription factor members.

		<b>activation mechanism</b>	<b>phenotype</b>
<b>ETV1</b>	early prostate cancer	chromosomal translocation and/or over-expression	invasion, migration
	triple negative breast cancer; Her2+ breast cancer	coactivation with Ras signaling and/or Her2 signaling	invasion, migration growth
	melanoma	amplification	invasion
<b>ETV4</b>	metastatic prostate cancer	coactivation with Ras, PI3 kinase signaling	invasion, migration
	triple negative or Her2+ breast cancer	coactivation with Ras and/or Her2 signaling	invasion, migration growth
	pancreatic cancer	coactivation with ERK signaling	invasion, migration
<b>ETV5</b>	head and neck cancer	top 1% of genes amplified	N/A

### 1.5 The Challenge of Drugging Protein-Protein Interactions

Although protein-protein interactions are sought after drug targets, there are limitations in discovery. Protein-protein interactions, unlike enzymes, often do not have well-defined binding cavities. The surface area plays an important role in protein-protein interactions, with surface areas ranging from  $500\text{\AA}^2$  to greater than  $5000\text{\AA}^2$ . This category of interactions have a range of binding affinities. For example, the CBP-KIX domain, a 90 residue domain, has a small surface area and binds the c-Myb transactivation domain with low binding affinity in the single-digit micromolar range. In contrast, the MDM2 protein binds p53 transcription factor with high affinity of approximately 60 nM.<sup>21</sup>

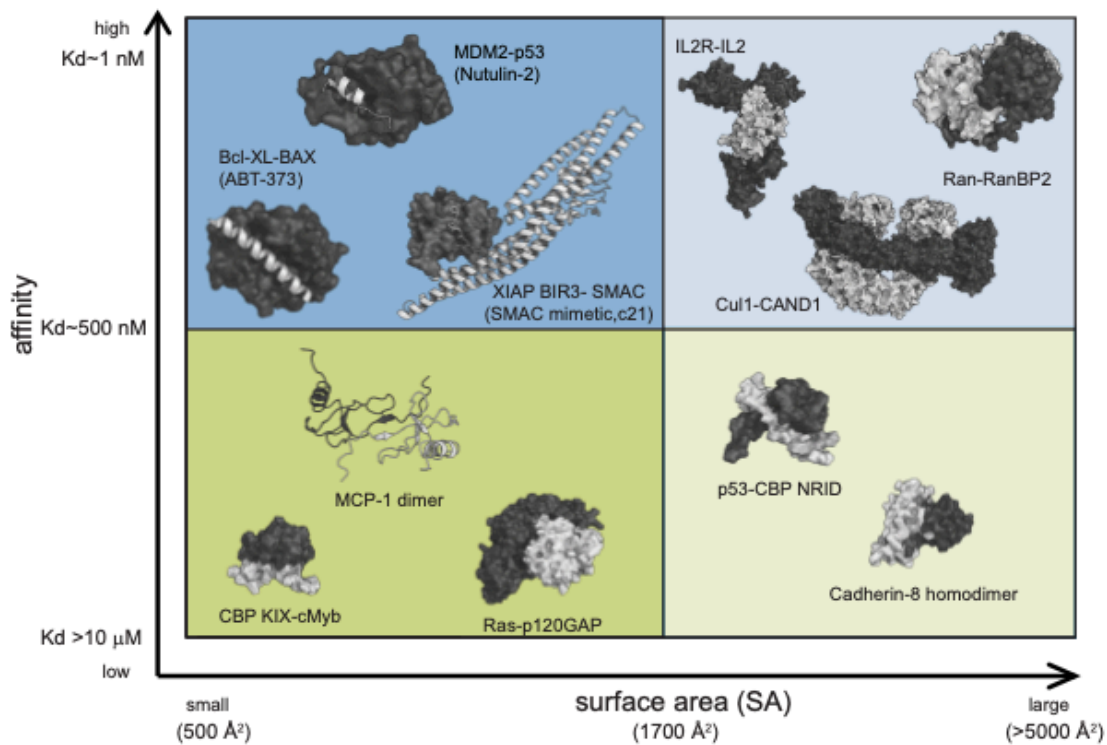


**Figure 1.3** The surface area-affinity relationship. Protein-protein interactions' surface area varies based on the size of the protein interface and affinity is proportional to this change.

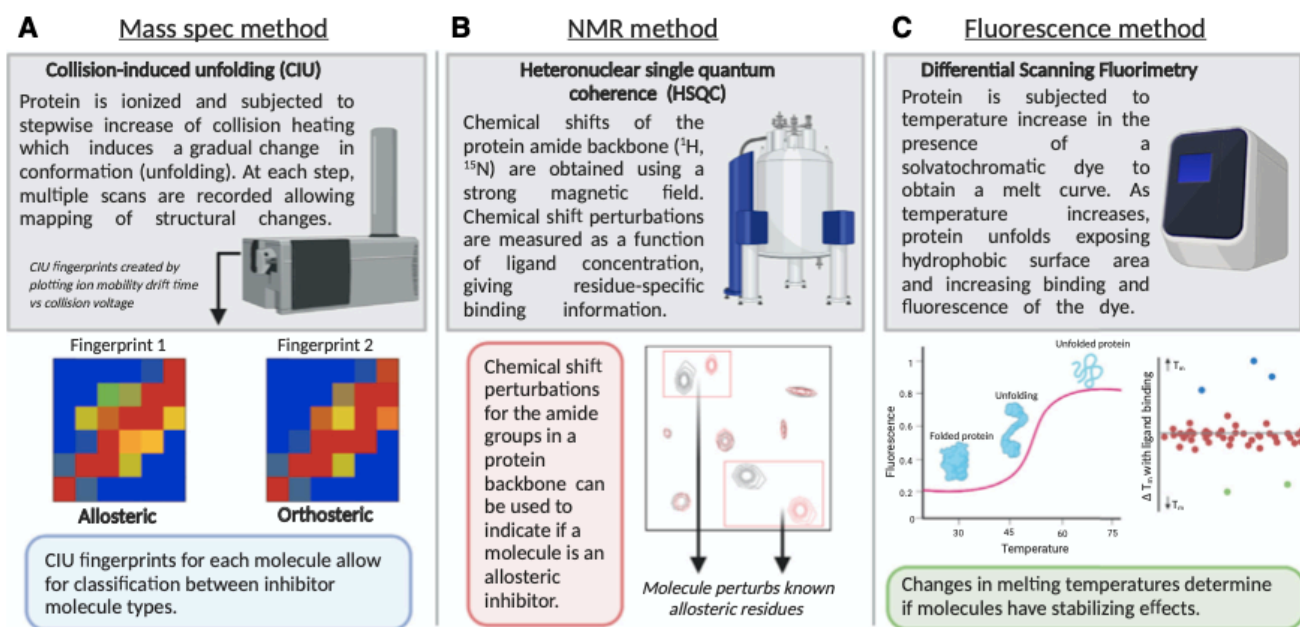
Another difficulty of targeting protein-protein interactions is that many lack topology. In the case of Med25-AcID, the original structural studies suggested that the  $\beta$ -barrel has the bulk of the contacts with cognate transcriptional activators and this surface is not only large but largely featureless. In other words, there are not binding grooves or clefts that could accommodate small molecules. An additional complication is that coactivators such as Med25 are involved in forming short-lived contacts where the dynamic characteristics of the protein accommodate this binding event. The dynamic regions usually include disordered loop regions and helix substructures which are thought to contribute to allosteric communication effects in protein-protein interactions. This as a result that makes small molecule discovery difficult.



There are emerging technologies that have been used in targeting dynamic proteins. Techniques such as mass spectrometry, NMR, and fluorescence based methods are examples that have been used to identify small molecule modulators.<sup>11</sup> Identifying small molecule modulators are probes that bind proteins that cause allosteric effects. Allosteric modulators are particularly desirable for dynamic proteins such as coactivators because of their ability to capture different conformational states. This is useful because coactivators can bind with more than one partner and adopt conformations useful in expressing appropriate genes. Allosteric modulators thus will be powerful tools to regulate gene expression in disease states. For these reasons, screening or analysis methods that enable detection of conformational changes in the protein are particularly useful for identifying allosteric modulators of coactivators.

Heteronuclear single quantum coherence (HSQC) NMR spectroscopic methods can be used to detect conformational changes induced by small molecules by measuring chemical shift changes in the amide backbone or in particular side chains. Collision Induced Unfolding (CIU) involves Ion Mobility Mass Spectrometry (IM-MS) which rapidly detects conformation of proteins based upon stability and unfolding patterns by monitoring ions in gas phase. This method produces intensity fingerprints that are then compared between protein species. Lastly, differential scanning fluorimetry (DSF) reports on the conformation of proteins as well.<sup>34</sup> A fluorescent dye is incubated with your protein species of interest. The sample is then heated over a range of temperatures and the dye binds as temperature rises accompanied by protein unfolding. This in turn increases fluorescence signals. Thus, if a small molecule alters the stability of the protein of interest, this will be detected by a change in the observed melting temperature in DSF. While all

of these are valuable methods for studying dynamic proteins such as coactivators, it is only DSF that is easily formatted for high throughput screening. And, unlike the first two methods, structural models can only be obtained by follow-on experiments.

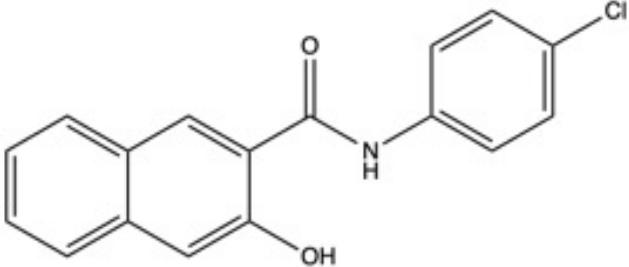


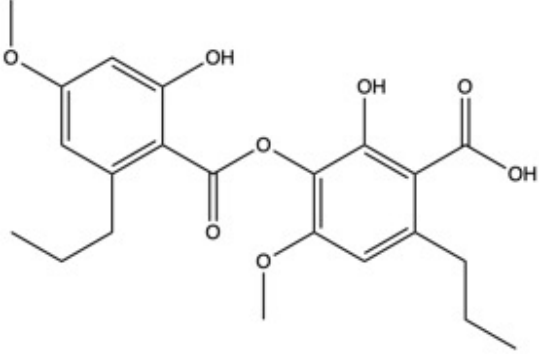
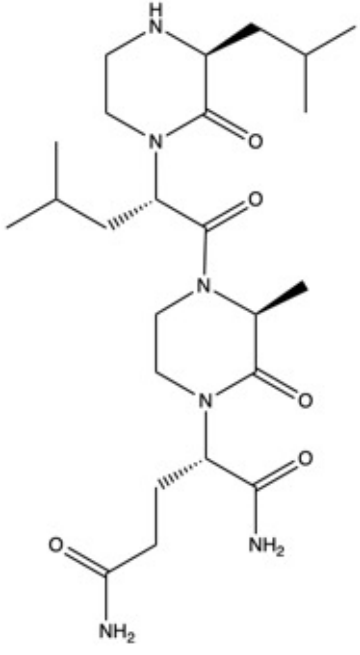
**Figure 1.4** Techniques used for small molecule discovery for dynamic proteins. (A) Collision-induced unfolding method maps structural changes by mass spectrometry. (B) NMR Methods monitors conformational changes caused by small molecules with protein backbone shifts. (C) DSF monitors small molecules ability to stabilize proteins of interest. This was used with the permission of the publisher.

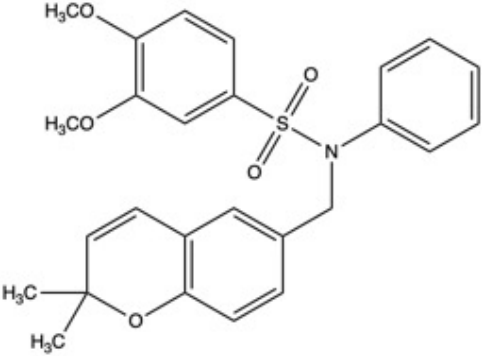
There are examples in which research groups have shown successful small molecules that target dynamic coactivator protein-protein interactions. The CBP/p300 master coactivator complex has more than one activator binding domain that has been targeted.<sup>8</sup> The KIX domain of the complex is capable of binding more than one activator using two surfaces. Natural products have yielded inhibitory effects when KIX is bound to activators MLL and pKID. Sekikaic acid which is a part of the depside family, produces these

results.<sup>18</sup> The c-Myb activator can bind KIX as well, and it is implicated in the development of leukemia. Naphthol inhibits c-Myb activity *in vitro* and *in vivo*.<sup>30</sup> Other domains such as Taz 1 have been targeted with inhibitors such as OHM1<sup>16</sup> and KCN1<sup>36</sup>. These target the HIF1 $\alpha$ -Taz1 interaction. These molecule serve as an example in the field that show some of the limited amount of small molecule inhibitors and the need to better understand the underlying principles of coactivator molecular recognition.<sup>4</sup>

**Table 1.3 Coactivator Protein Inhibitors**

Compound Name	Source	Interaction
Naphthol AS-E 	Mol Cancer Ther 2015, 14:1276-1285	KIX - c-Myb
Sekikaic acid	Angew. Chem. Int. Ed. 2012, 51: 11258 -11262	KIX-MLL & KIX-pKID

		
<p>OHM1</p> 	<p>PNAS. 2014, 111: 75 31-7536</p>	<p>Taz1 - Hif- 1<math>\alpha</math></p>

<p>KCN1</p> 	<p>Clin Cancer Res 2012, 18: 6623-6633</p>	<p>Taz1 - Hif- 1<math>\alpha</math></p>
---	--	---

## 1.6 Thesis Summary

The goal of this thesis work is to identify key principles of how Med25 interacts with binding partners and to identify small molecule fragments that target the coactivator. As outlined in Chapter 2, a study was carried out to define key binding characteristics of the Med25-AcID activator interaction. This was done by initially using fluorescence polarization and site directed mutagenesis to determine the binding sites of AcID's interacting activators. This was then followed by defining the contributions of electrostatics through salt changes and activator peptide mutations in maintaining binding affinity. The substructures of AcID were thought to be important players in activator recognition as a large number of charged residues are localized in these regions. This was further confirmed by molecular dynamic simulations. Described in Chapter 3, building from this theme a small molecule fragment library was screened against AcID using the Tethering technique. It was performed in a manner that isolated hits specific to the dynamic loop substructure of AcID. The screen yielded a fragment that stabilizes the AcID

domain that could be important in regulating binding activators which has been seen in literature with another coactivator protein.

## 1.7 Reference

1. Allen, Benjamin L., and Dylan J. Taatjes. "The Mediator Complex: A Central Integrator of Transcription." *Nature Reviews Molecular Cell Biology*, vol. 16, no. 3, Mar. 2015, pp. 155–66, doi:10.1038/nrm3951.
2. Asada, Shinichi, et al. "External Control of Her2 Expression and Cancer Cell Growth by Targeting a Ras-Linked Coactivator." *Proceedings of the National Academy of Sciences*, vol. 99, no. 20, Oct. 2002, p. 12747, doi:10.1073/pnas.202162199.
3. Baert, Jean-Luc, et al. "Expression of the PEA3 Group of ETS-Related Transcription Factors in Human Breast-Cancer Cells." *International Journal of Cancer*, vol. 70, no. 5, 1997, pp. 590–97, doi:10.1002/(SICI)1097-0215(19970304)70:5<590::AID-IJC17>3.0.CO;2-H.
4. Breen, Meghan E., and Anna K. Mapp. "Modulating the Masters: Chemical Tools to Dissect CBP and P300 Function." *Current Opinion in Chemical Biology*, vol. 45, 2018, pp. 195–203, doi:https://doi.org/10.1016/j.cbpa.2018.06.005.
5. Brzovic, Peter S., et al. "The Acidic Transcription Activator Gcn4 Binds the Mediator Subunit Gal11/Med15 Using a Simple Protein Interface Forming a Fuzzy Complex." *Molecular Cell*, vol. 44, no. 6, Elsevier, Dec. 2011, pp. 942–53, doi:10.1016/j.molcel.2011.11.008.

6. Conaway, Ronald C., and Joan Weliky Conaway. "Origins and Activity of the Mediator Complex." *Seminars in Cell & Developmental Biology*, vol. 22, no. 7, Sept. 2011, pp. 729–34. *PubMed*, doi:10.1016/j.semcdb.2011.07.021.
7. Currie, Simon L., et al. "ETV4 and AP1 Transcription Factors Form Multivalent Interactions with Three Sites on the MED25 Activator-Interacting Domain." *Journal of Molecular Biology*, vol. 429, no. 20, Oct. 2017, pp. 2975–95, doi:10.1016/j.jmb.2017.06.024.
8. Dyson, H. Jane, and Peter E. Wright. "Role of Intrinsic Protein Disorder in the Function and Interactions of the Transcriptional Coactivators CREB-Binding Protein (CBP) and P300." *Journal of Biological Chemistry*, vol. 291, no. 13, Mar. 2016, pp. 6714–22, doi:10.1074/jbc.R115.692020.
9. El Khattabi, Laila, et al. "A Pliable Mediator Acts as a Functional Rather Than an Architectural Bridge between Promoters and Enhancers." *Cell*, vol. 178, no. 5, Elsevier, Aug. 2019, pp. 1145-1158.e20, doi:10.1016/j.cell.2019.07.011.
10. Fregoso, Mariana, et al. "DNA Repair and Transcriptional Deficiencies Caused by Mutations in the Drosophila P52 Subunit of TFIIH Generate Developmental Defects and Chromosome Fragility." *Molecular and Cellular Biology*, vol. 27, no. 10, May 2007, pp. 3640–50. *PubMed*, doi:10.1128/MCB.00030-07.
11. Garlick, Julie M., and Anna K. Mapp. "Selective Modulation of Dynamic Protein Complexes." *Cell Chemical Biology*, vol. 27, no. 8, Elsevier, Aug. 2020, pp. 986–97, doi:10.1016/j.chembiol.2020.07.019.

12. Hsu, Tun-Chieh, et al. "Deactivation of TBP Contributes to SCA17 Pathogenesis." *Human Molecular Genetics*, vol. 23, no. 25, Dec. 2014, pp. 6878–93, doi:10.1093/hmg/ddu410.
13. Kornberg, Roger D. "Mediator and the Mechanism of Transcriptional Activation." *Trends in Biochemical Sciences*, vol. 30, no. 5, Elsevier, May 2005, pp. 235–39, doi:10.1016/j.tibs.2005.03.011.
14. ---. "The Molecular Basis of Eukaryotic Transcription." *Proceedings of the National Academy of Sciences*, vol. 104, no. 32, Aug. 2007, p. 12955, doi:10.1073/pnas.0704138104.
15. Landrieu, Isabelle, et al. "Characterization of ERM Transactivation Domain Binding to the ACID/PTOV Domain of the Mediator Subunit MED25." *Nucleic Acids Research*, vol. 43, no. 14, Aug. 2015, pp. 7110–21, doi:10.1093/nar/gkv650.
16. Lao, Brooke Bullock, et al. "In Vivo Modulation of Hypoxia-Inducible Signaling by Topographical Helix Mimetics." *Proceedings of the National Academy of Sciences*, vol. 111, no. 21, May 2014, p. 7531, doi:10.1073/pnas.1402393111.
17. Lee, Min-Sung, et al. "Structural Basis for the Interaction between P53 Transactivation Domain and the Mediator Subunit MED25." *Molecules*, vol. 23, no. 10, 2018, doi:10.3390/molecules23102726.
18. Majmudar, Chinmay Y., et al. "Sekikaic Acid and Lobaric Acid Target a Dynamic Interface of the Coactivator CBP/P300." *Angewandte Chemie International Edition*, vol. 51, no. 45, 2012, pp. 11258–62, doi:10.1002/anie.201206815.



19. Malik, Sohail, and Robert G. Roeder. "The Metazoan Mediator Co-Activator Complex as an Integrative Hub for Transcriptional Regulation." *Nature Reviews Genetics*, vol. 11, no. 11, Nov. 2010, pp. 761–72, doi:10.1038/nrg2901.
20. Mapp, Anna K., and Aseem Z. Ansari. "A TAD Further: Exogenous Control of Gene Activation." *ACS Chemical Biology*, vol. 2, no. 1, American Chemical Society, Jan. 2007, pp. 62–75, doi:10.1021/cb600463w.
21. Michael, Dan, and Moshe Oren. "The P53–Mdm2 Module and the Ubiquitin System." *Seminars in Cancer Biology*, vol. 13, no. 1, 2003, pp. 49–58, doi:https://doi.org/10.1016/S1044-579X(02)00099-8.
22. Mitchell, D. C., et al. "Transcriptional Regulation of KiSS-1 Gene Expression in Metastatic Melanoma by Specificity Protein-1 and Its Coactivator DRIP-130." *Oncogene*, vol. 26, no. 12, Mar. 2007, pp. 1739–47, doi:10.1038/sj.onc.1209963.
23. O'Rawe, Jason A., et al. "TAF1 Variants Are Associated with Dysmorphic Features, Intellectual Disability, and Neurological Manifestations." *The American Journal of Human Genetics*, vol. 97, no. 6, Elsevier, Dec. 2015, pp. 922–32, doi:10.1016/j.ajhg.2015.11.005.
24. piskacek, martin. "9aaTADs Mimic DNA to Interact with a Pseudo-DNA Binding Domain KIX of Med15 (Molecular Chameleons)." *Nature Precedings*, Nov. 2009, doi:10.1038/npre.2009.3939.1.
25. Sela, Dotan, et al. "Role for Human Mediator Subunit MED25 in Recruitment of Mediator to Promoters by Endoplasmic Reticulum Stress-Responsive Transcription Factor ATF6 $\alpha$ ." *Journal of Biological Chemistry*, vol. 288, no. 36, Sept. 2013, pp. 26179–87, doi:10.1074/jbc.M113.496968.

26. Spaeth, Jason M., et al. "Mediator and Human Disease." *Seminars in Cell & Developmental Biology*, vol. 22, no. 7, Sept. 2011, pp. 776–87. *PubMed*, doi:10.1016/j.semcdb.2011.07.024.
27. Stevens, Jennitte L., et al. "Transcription Control by E1A and MAP Kinase Pathway via Sur2 Mediator Subunit." *Science*, vol. 296, no. 5568, Apr. 2002, p. 755, doi:10.1126/science.1068943.
28. Triezenberg, S. J., et al. "Functional Dissection of VP16, the Trans-Activator of Herpes Simplex Virus Immediate Early Gene Expression." *Genes & Development*, vol. 2, no. 6, June 1988, pp. 718–29, doi:10.1101/gad.2.6.718.
29. Tuttle, Lisa M., et al. "Mediator Subunit Med15 Dictates the Conserved 'Fuzzy' Binding Mechanism of Yeast Transcription Activators Gal4 and Gcn4." *BioRxiv*, Jan. 2019, p. 840348, doi:10.1101/840348.
30. Uttarkar, Sagar, et al. "Naphthol AS-E Phosphate Inhibits the Activity of the Transcription Factor Myb by Blocking the Interaction with the KIX Domain of the Coactivator P300." *Molecular Cancer Therapeutics*, vol. 14, no. 6, June 2015, p. 1276, doi:10.1158/1535-7163.MCT-14-0662.
31. Uversky, Vladimir N., et al. "Intrinsically Disordered Proteins in Human Diseases: Introducing the D2 Concept." *Annual Review of Biophysics*, vol. 37, no. 1, Annual Reviews, May 2008, pp. 215–46, doi:10.1146/annurev.biophys.37.032807.125924.
32. Verger, Alexis, et al. "The Mediator Complex Subunit MED25 Is Targeted by the N-Terminal Transactivation Domain of the PEA3 Group Members." *Nucleic Acids Research*, vol. 41, no. 9, May 2013, pp. 4847–59, doi:10.1093/nar/gkt199.

33. Vojnic, Erika, et al. "Structure and VP16 Binding of the Mediator Med25 Activator Interaction Domain." *Nature Structural & Molecular Biology*, vol. 18, no. 4, Apr. 2011, pp. 404–09, doi:10.1038/nsmb.1997.
34. Wu, Taia, et al. "Three Essential Resources to Improve Differential Scanning Fluorimetry (DSF) Experiments." *BioRxiv*, Jan. 2020, p. 2020.03.22.002543, doi:10.1101/2020.03.22.002543.
35. Yang, Fajun, et al. "An ARC/Mediator Subunit Required for SREBP Control of Cholesterol and Lipid Homeostasis." *Nature*, vol. 442, no. 7103, Aug. 2006, pp. 700–04, doi:10.1038/nature04942.
36. Yin, Shaoman, et al. "Arylsulfonamide KCN1 Inhibits *In Vivo* Glioma Growth and Interferes with HIF Signaling by Disrupting HIF-1 $\alpha$  Interaction with Cofactors P300/CBP." *Clinical Cancer Research*, vol. 18, no. 24, Dec. 2012, p. 6623, doi:10.1158/1078-0432.CCR-12-0861.

## Chapter 2.

### Interrogating the Coactivator Med25-Activator Interaction<sup>1</sup>

#### 2.1 Abstract

Transcriptional coactivators are highly dynamic proteins that assist in the initiation of gene expression. The hub protein and coactivator Med25 has the ability to recognize many different transcription factors as part of its role in transcriptional initiation. It has been shown to associate with transcription factors such as herpes simplex virus VP16 (viral infection), Erm (cancer metastasis), and ATF6 $\alpha$  (unfolded protein response). It also contains a unique structural fold in comparison to other coactivator proteins. Most coactivator proteins contain a helix bundle motif, while Med25 uses a stable  $\beta$ -barrel core flanked by helix bundles and flexible loop regions. Thus, a key question in the field has been if the uniquely folded Med25 **A**ctivator **I**nteraction **D**omain (AcID) protein-protein interactions form via mechanisms distinct from the canonical coactivator structures. Chapter 2 outlines our findings that electrostatics and dynamic substructures are essential for the affinity and specificity of Med25's interaction with **T**ranscriptional **A**ctivation **D**omains (TADs). This data shows the activator ATF6 $\alpha$  and Erm bind in

---

<sup>1</sup> Portions of this chapter are from "Conservation of coactivator engagement mechanism enables small-molecule allosteric modulators" A. R. Henderson, M.J. Henley, **N. J. Foster**, A.L. Peiffer, M.S. Beyersdorf, K.D. Stanford, S. M. Sturlis, B. M. Linhares, Z.B. Hill, J. A. Wells, T. Cierpicki, C. L. Brooks III, C.A. Fierke, A. K. Mapp. *Proc. Natl. Acad. Sci. USA* **2018** 115, 8960-65.

different locations; charged residues of this coactivator-activator complex maintain interaction; and activators stabilize AcID substructures.

## **2.2 Introduction**

### Mediator Subunit Med25

The Med25 subunit is a part of the tail region of the Mediator coactivator complex (Figure 2.1A). This subunit is composed of three domains (Figure 2.1B). The VWA domain located on the N-terminus interacts with the other subunits of the Mediator complex. The C-terminus contains the motif LXXL noted for binding nuclear receptors such as the retinoid receptor. The activator interaction domain (AcID) binds different transcription factors and in this way Med25 can bridge transcription factors and the overall Mediator complex. The AcID domain uses two binding sites labeled the H1 and H2 face to engage transcription factors (Figure 2.1C). Although there are no crystal structures of Med25-AcID, there are reported NMR structures of the AcID domain.<sup>1</sup> Such structural information allows for further analyses of AcID and its engagement with activators.

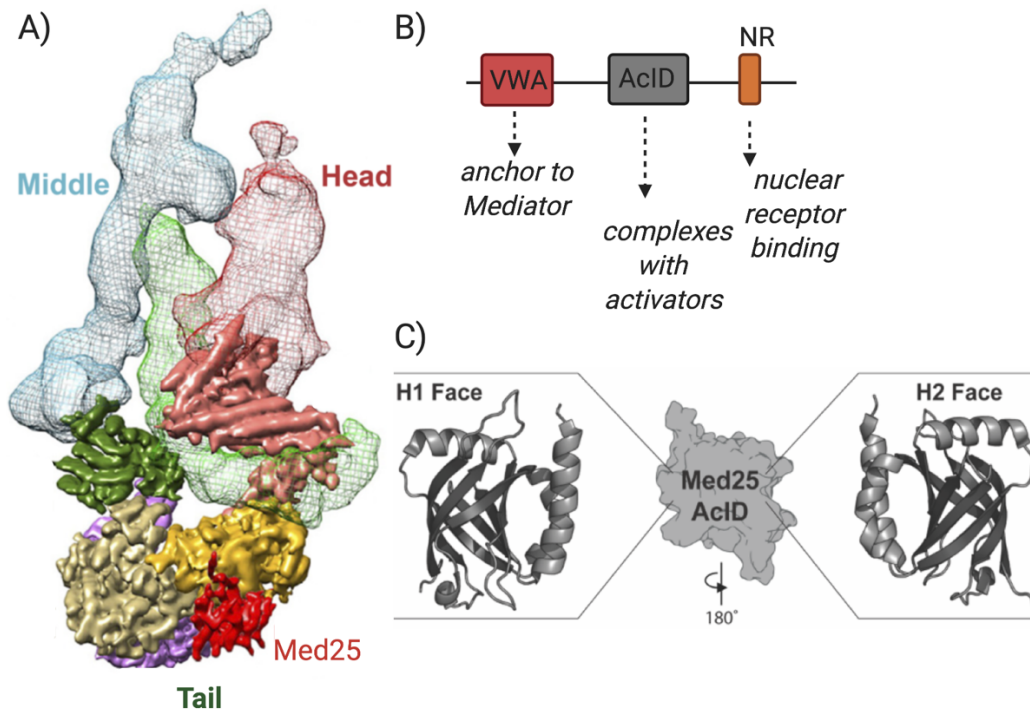


**Figure 2.1** The Mediator's Subunit Med25 (A) Mediator structure that highlights the tail region that contains Med25.<sup>7</sup> (B) The three domains of Med25 are displayed (C) The Activator Interaction domain's two binding surfaces.

Through its ability to engage with a variety of activator binding partners by way of AcID, Med25 regulates a diverse set of genes. Activator ERM, which belongs to the PEA3 subfamily of Ets transcription factors, complexes with AcID to regulate matrix metalloprotease protein-2 (MMP-2) that is involved in cancer metastasis.<sup>11,25,5</sup> ATF6 $\alpha$  is another prominent transcription factor that is dependent upon AcID for function, in this case upregulation of the cellular stress response.<sup>18</sup> Perhaps the best studied binding partner is the viral activator VP16, a protein from herpes simplex that hijacks coactivators such as Med25 to upregulate the immediate-early viral genes upon infection.<sup>9</sup>

VP16 was the first binding partner characterized in complex with Med25. VP16 contains an approximately 50 residue transcriptional activation domain that it uses to complex with coactivators.<sup>14,26</sup> In the case of Med25-AcID, two studies published

simultaneously in 2011 showed that the VP16 activation domain wraps around the  $\beta$ -barrel, contacting both binding surfaces within AcID. As later shown by our lab and others, the N-terminal and C-terminal halves of VP16 can bind independently to AcID. The N-terminal half is termed VP16H1 and engage one surfaces the appropriately named H1 binding surface of AcID. Conversely, the C-terminal half called VP16H2 interacts with the H2 Med25-AcID binding surface (Figure 2.1C). Subsequent NMR studies by Verger and co-workers revealed that the ERM transcriptional activation domain interacts with the H1 surface. However, although the Med25-AcID dependence of ATF6 $\alpha$  was well-established, the location of its binding was not known. Thus, there were questions as to the relevance of the H2 binding surface.

#### Med25-Dependent Activators

**VP16:** 438 -ALDDFDLMDLGDGDSPPGPGPFTPHDSAPYGALDMADFEFEQMFTDALGIDEYGG -490

**ERM:** 38-DLAHDSEELFQDLSQLQEAWLAEAQVPDDEQ-68

**ATF6 $\alpha$ :** 40 -DTDELQLEAANETYENNFDNLDFDL-66

A notable aspect of Med25 AcID-activator complexes is their relatively high affinity.<sup>13</sup> For example, the well-studied KIX motif of the coactivator CBP interacts with its cognate activators with  $K_D$ s ranging from 1-100  $\mu$ M whereas Med25 activator  $K_D$ s are in the nanomolar regime (VP16: 60 nM; ERM: 590 nM).<sup>8</sup> Affinity and specificity for activator-coactivator complexes are typically attributed to interactions between hydrophobic amino acids, as well as hydrogen bonding. For example, mutation of Trp57 in ERM reduces affinity for AcID >10-fold. There are indications that electrostatic interactions may also play a role in binding strength. Med25-AcID is overall positively charged (7.2) and the positively charged residues are largely located in the flexible loop regions (Table 2.1). Other known coactivators are positively charged as well. Conveniently, the activator-binding partners are amphipathic and negatively charged. For example, the Taz1 domain

of CBP coactivator complex is +10.2 in charge while its complementing binding activators HIF1- $\alpha$  and CITED2 are -5.1 and -7.<sup>27,3,4</sup> Further, in this latter example, the electrostatic contacts are important for essential allosteric communication between binding sites.<sup>21,19</sup> For these reasons, we hypothesized that electrostatic contacts might play an important role in affinity and perhaps specificity of Med25 AcID-activator complexes.

**Table 2.1 The Net Charge of Activator Binding Proteins**

<b>Activator Binding Domains (ABDs)</b>	<b>Net Charge</b>	<b>PDB</b>
Med25 AcID	7.2	2XNF
CBP Taz 1	10.2	1U2N
CBP Taz 2	18.9	3IO2
CBP KIX	3.5	4I9O
TBP	15.9	1CDW
CBP IBiD	5.0	1ZOQ

The misregulation of the Erm-Med25 AcID and ATF6 $\alpha$ -Med25 AcID PPIs are implicated in breast and prostate cancer. Despite considerable interest in these PPIs, however, there were no reported synthetic modulators. Med25-AcID in particular is challenging to target due to the large, featureless binding surfaces with which the activators interact and the lack of a more molecular-level understanding of how they interact. Further, although we and others have found that in the case of helical coactivators the loop regions are especially important for molecular recognition, literature data suggested that this might not be the case for Med25 due to its distinct structure.<sup>6,20</sup> So, the goal in the work of this



chapter was to test if electrostatics and dynamic substructures were similarly important for Med25 as displayed in other coactivator-activator binding events.

## 2.3 Results & Discussion

### Dissection of Activator Binding Location

Coactivators bind intrinsically disordered transactivation domains that are heavily involved in disease.<sup>24</sup> Disordered activator regions interact on separate surfaces within coactivator hub proteins that communicate to express a desired gene. Med25-AcID was previously shown to have discrete binding surfaces labeled H1 and H2. In addition, VP16 and Erm were known to bind both surfaces in a particular location, but it was unknown where ATF6 $\alpha$  bound within the domain. To address this, we used a combination of mutagenesis and binding experiments to uncover where activator ATF6 $\alpha$  binds on the protein.

First, to identify the binding site of ATF6 $\alpha$ , we measured the chemical shift changes in each activator-AcID complex via <sup>1</sup>H, <sup>15</sup>N-HSQC NMR titration experiments with ERM(38-68) and ATF6 $\alpha$ (40-66) in the presence of <sup>15</sup>N-labeled Med25 AcID. The amide proton perturbation patterns measured for the activator•AcID complexes suggest a different binding mode for ERM and ATF6 $\alpha$ . ERM binding predominantly led to perturbations at residues on the H1 surface of AcID, in agreement with the model in which it preferentially interacts at that site. In contrast, interaction with ATF6 $\alpha$  lead to significant chemical shifts changes on the H2 binding surface. ATF6 $\alpha$ -induced shifts of residues Q456, M470, and H474 which were also affected to varying degrees by VP16 and largely unaltered by ERM.

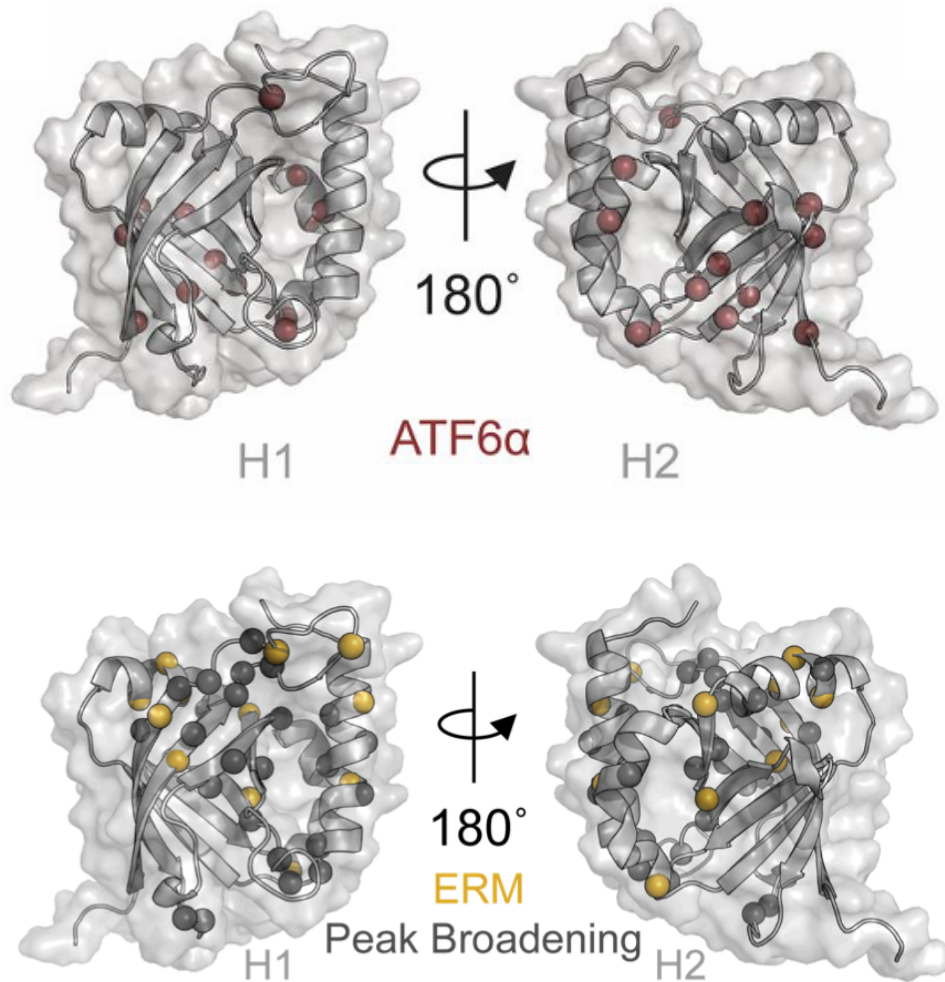



**Figure 2.2** Erm and ATF6 $\alpha$  bind opposite surfaces in NMR studies. Results of chemical shift perturbation experiments superimposed upon the Med25-AcID structure (PDB 2XNF). Residues displaying chemical shift perturbation greater than 2 SD upon Erm and ATF6 $\alpha$  binding are depicted in rust and yellow spheres. Experiments were done by Dr. Andrew Henderson and Dr. Brian Linhares.

Consistent with ATF6 $\alpha$  and ERM interacting on opposing sides of AcID, mutations introduced on one or the other of the binding surfaces produced distinct effects. H1 mutations R538E, K411E, and Q451E inhibit ERM binding while ATF6 $\alpha$  is largely unaffected. In contrast, H2 mutations R466D and M523E significantly inhibit ATF6 $\alpha$  with minimal impact on ERM binding. Taken together these data indicate that ATF6 $\alpha$  binds on

the H2 binding surface of Med25-AcID, opposite the site of ERM. Further, the distinct but overlapping chemical shift patterns observed upon binding of each of the activators to Med25 suggest several unique binding modes accommodated within AcID. This is analogous to helical activator binding domains such as GACKIX of CBP/p300, a three-helix bundle that contains at least two activator binding sites.

		Fold Change $K_D$				
		Med25 Mutation				
		R538E	K411E	Q451E	R466D	M523E
ERM		$5.9 \pm 0.4$	$4.2 \pm 0.1$	$3.0 \pm 0.7$	$0.9 \pm 0.1$	$1.2 \pm 0.7$
ATF6 $\alpha$		$1.7 \pm 0.3$	$1.0 \pm 0.1$	$1.4 \pm 0.2$	$6.3 \pm 0.1$	$9.0 \pm 2$

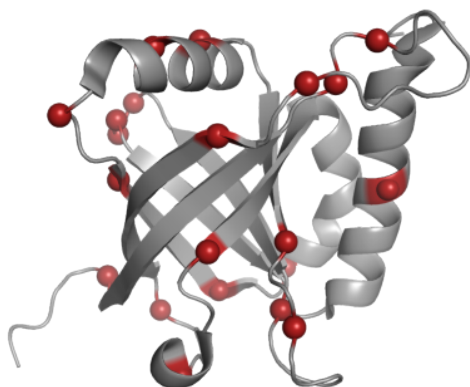


**Figure 2.3** Mutagenesis shows ATF6 $\alpha$  engages the H2 binding surface. Results of direct binding experiments with fluorescein-labeled activators and the indicated mutants of Med25 AcID as measured by fluorescence polarization expressed the fold change relative to the dissociation constant of each activator for the WT AcID. The indicated error is propagated from three independent dissociation constant measurements. Binding experiments were carried out collaboratively by Dr. Andrew Henderson, **Nicholas Foster**, Dr. Matthew Beyersdorf, Kevon Stanford, and Dr. Steven Sturlis.

#### The Role of Electrostatics in Activator Interactions with Med25-AcID

As outlined in the Med25 AcID has a large number of positive charged residues located within the domain (Figure 2.4 - top). These residues are mostly located in its dynamic

loop and helix substructures. The loop regions of the domain contain 10 positive charged residues, where 5 (K411, K413, K422, H502, and R509) are on the H1 face and 3 (K518, K519, and K520) on the H2 face. The remaining 2 (H435 and K440) are in the loop region spanning the bottom of the domain. The  $\beta$ -barrel has only 4 positive residues (R425, K447, H474, and H499). In contrast, its binding activators are most negatively charged (Figure 2.4 - bottom). AcID's binding activators have a net charge that ranges from -7 to -13.9. These characteristics suggest that electrostatic contacts are important for transcription factor binding to Med25 and could also contribute to selectivity relative to other coactivators. Experiments were thus designed to test this hypothesis.



Activator Peptide	Sequence	Net Charge
ERM <sub>38-72</sub>	DLAHDSEELFQDLSQLQEAWLAEAQVPDDEQFVPD	-10.9
ATF6 $\alpha$ <sub>40-66</sub>	DTDELQLEAANETYENNFDNLDFDLDL	-10
VP16 <sub>438-490</sub>	ALDDFDLDM LGDGSPGPGFTPHDSAPYGALDM ADFEFEQMFTDALGIDEYGG	-13.9
CBP <sub>20-44</sub>	PGFSANDSTDFGSLFDLENDLPDEL	-7

**Figure 2.4** Positive Residues of AcID and Negative Residues of Binding Activators. (top) shows the positive residues of the Med25-AcID shown in red.(bottom) shows the sequence and net charge of binding activators.

The most common strategy to test the role of electrostatic interactions in binding is to change the nature and concentration of salt present in buffer solutions. Salts within buffers are able to interact directly and indirectly with proteins in solution with varying strength, depending on the nature of the constituent ions and their concentration. The Hofmeister series of cations and anions was originally identified from studies of protein precipitation and unfolding<sup>10</sup>. More recent studies have revealed that in many cases ions can bind charged side chain residues of a protein or peptide, producing a shielding effect that thus can affect binding (Figure2.5).

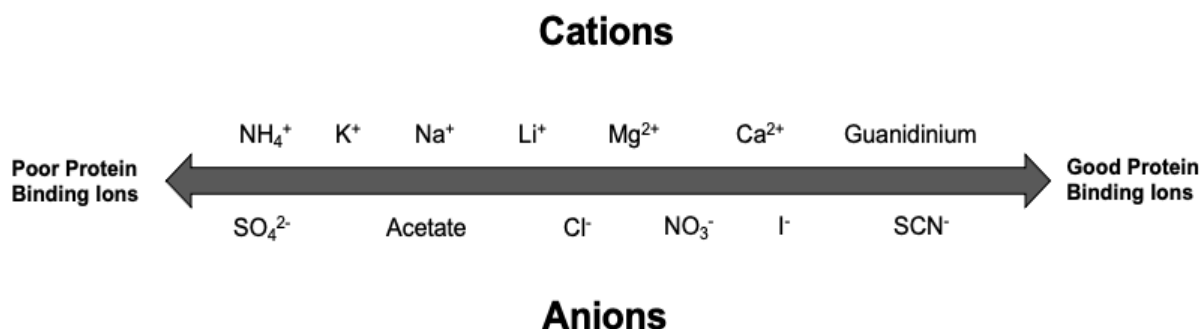
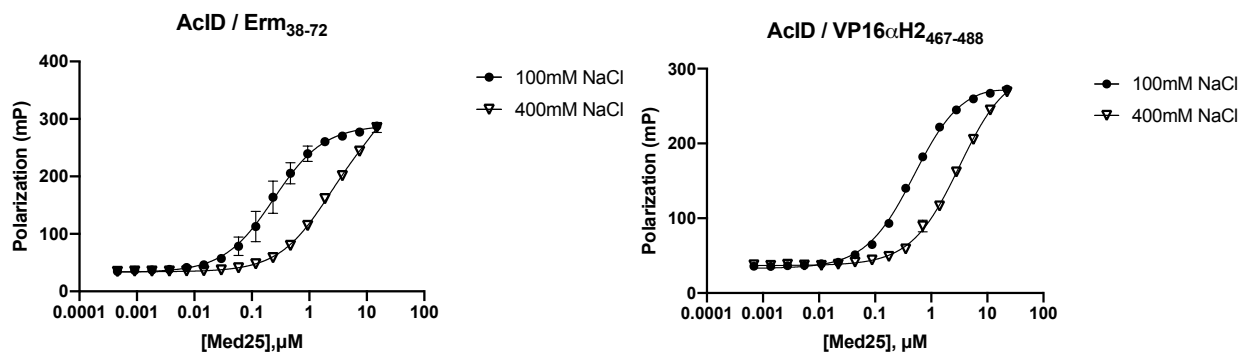


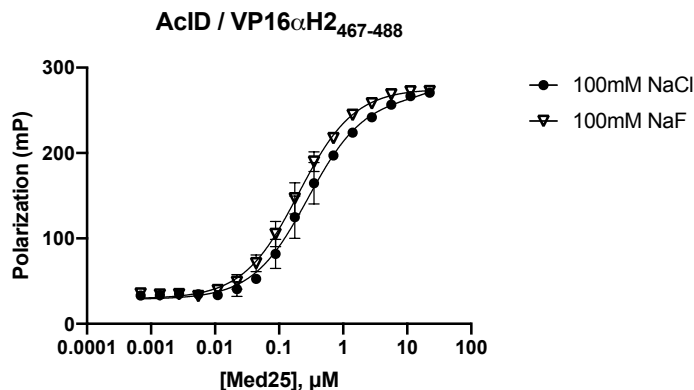
**Figure 2.5** The Hofmeister Series. Starting from the left identifies the poor binding ions of proteins and ions furthest to the right show the best binding ions of proteins

After considering the Hofmeister series, binding experiments were first carried out that increased the concentration of sodium chloride in the assay buffer.<sup>15,16</sup> Standard binding assay buffer contains 100 mM sodium chloride which is close to normal cell concentrations and 10 mM sodium phosphate. Thus, if electrostatic interactions play an important role in binding then higher sodium chloride concentrations should decrease the stability of the complex and binding affinity. Med25-AcID binds the activator peptide

Erm<sub>38-72</sub> with an  $K_D$  value of 0.2  $\mu\text{M}$  and this decreases affinity 10-fold. The activator peptide VP16 $\alpha$ H2<sub>467-488</sub> interacts with the opposite face (H2) and shows a 6.4-fold decrease upon increasing NaCl concentrations to 400 mM. In contrast, the presence of 100 mM NaF shows minimal change in binding affinity of activator VP16 $\alpha$ H2<sub>467-488</sub>. Thus, electrostatic interactions at both the H1 and H2 binding surfaces appear relevant.



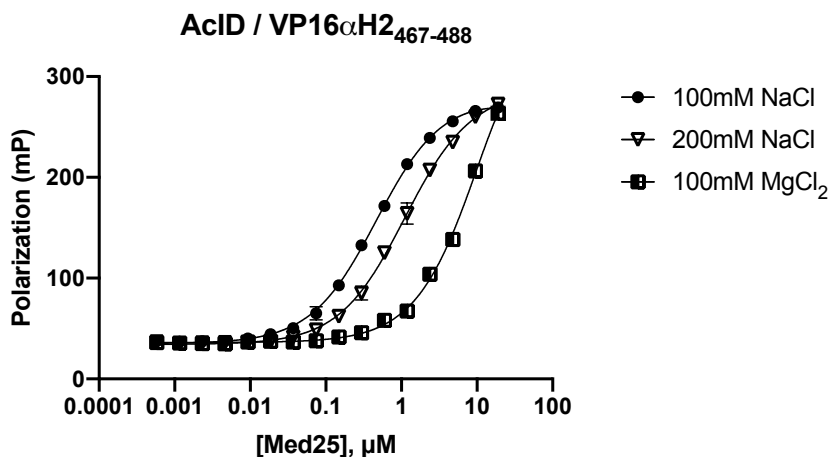
	100 mM NaCl	400 mM NaCl
ERM <sub>38-72</sub>	0.2 ± 0.04	2.0 ± 0.2
VP16 <sub>437-488</sub>	0.5 ± 0.03	3.2 ± 0.3



Salts	$K_D$ Values ( $\mu\text{M}$ )
100 mM NaCl	0.3 ± 0.05
100 mM NaF	0.2 ± 0.02

**Figure 2.6** Salt anions change activator affinity. Measurements were taken in fluorescence polarization experiments. Each value is the average of at least three independent binding experiments with the indicated error (SDOM).

The size of ions was considered as well. There is a correlation between the size of the shielding ion and its effect on activator binding. Other salts were used in comparison to NaCl. MgCl<sub>2</sub> was used because it produces divalent Mg<sup>2+</sup> ions that bind better to negatively charged residues than Na<sup>+</sup>. The presence of MgCl<sub>2</sub> decreases VP16 $\alpha$ H2<sub>467-488</sub> binding by 13-fold indicating that it is better shielded by MgCl<sub>2</sub> and, further, that the negatively charged residues of the activator peptide play a key role in the affinity for Med25 AcID.

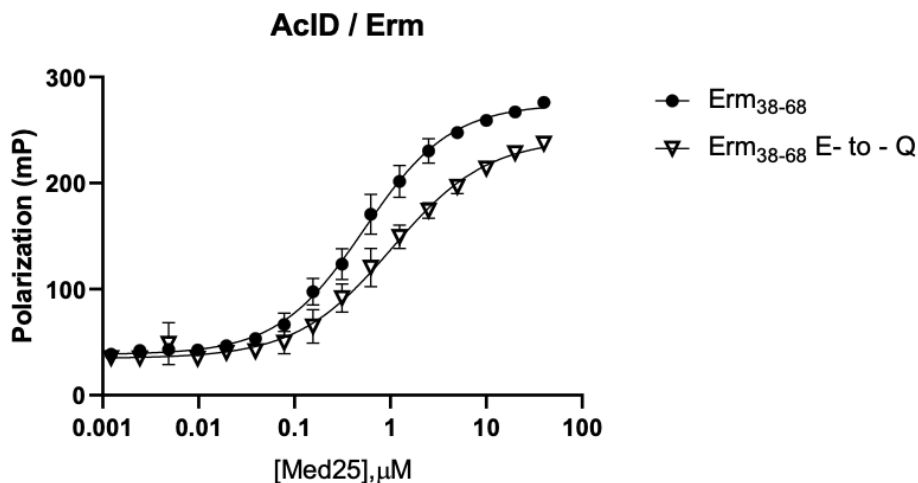


Salts	K <sub>D</sub> Values (μM)
100 mM NaCl	0.5 ± 0.03
200 mM NaCl	1.1 ± 0.1
100 mM MgCl <sub>2</sub>	13.0 ± 5.0

**Figure 2.7** Salt cation size changes activator affinity. Measurements were taken through fluorescence polarization experiments.

To further understand how electrostatics guide interaction, point mutations were implemented within the activator peptide of ERM<sub>38-68</sub> and binding affinities were

measured. This included mutating the negatively charged glutamic acid residues of the sequence to glutamine residues. This reduces the peptide charge from -9.9 to -4.9. The affinities were lowered by 2-fold.



	$K_D$ Values ( $\mu\text{M}$ )
ERM <sub>38-68</sub>	$0.53 \pm 0.08$
ERM <sub>38-68</sub> E - to - Q	$1.0 \pm 0.3$



**Figure 2.8.** Erm soft mutations alter affinity. All glutamic acid residues were mutated to glutamine residue. Binding experiments were measured through fluorescence polarization.

Taken together, these data demonstrate that it is not just hydrophobic interactions that contribute to Med25-activator interactions. Further, they are key at both the H1 and H2 binding surfaces. Increases in salt concentration inhibited binding for both ERM and the H2-binding half of VP16. This was further confirmed by soft mutations within ERM that removed charge and led to a 2-fold attenuation in binding affinity for Med25. These results are particularly interesting because nearly all of the charged residues in Med25 occur



outside the  $\beta$ -barrel binding surfaces that are reported to be the primary contacts for activator-binding surfaces.

## 2.4 Conclusions

Perhaps the most significant results that emerged from the studies in this chapter is the influential role of electrostatic contacts on the strength of Med25 AcID-activator complexes. As shown the second half of the work, activators that bind to either the H1 (ERM) or H2 (VP16(467-488)) are impacted significantly by either neutralizing mutations or increasing salt concentrations. This was somewhat surprising because the canonical view of activator-coactivator complexes is that they are driven by hydrophobic contacts and because the previously identified activator binding surfaces of Med25-AcID are largely hydrophobic, with the charged residues residing on adjacent loops and helices. To address this conundrum, colleague Amanda Peiffer carried out a computational study of activator-Med25 AcID complexes to develop a structural model. To do this, all-atom molecular dynamics simulations were carried out using implicit solvent models (GBSW) and with temperature replica exchange in CHARMM.<sup>22</sup> Simulations were performed on both unbound Med25-AcID and a model of this protein in which the VP16(438-454)<sub>G450C</sub> is covalently linked at C506. To identify the substructures most stabilized upon binding, the root-mean-square fluctuations (RMSF) for each residue were calculated from the resulting trajectories (Figure 2.9A and 2.9B). In these figures, the line color reflects the range of motion of each residue. In the unbound structure (Figure 2.9A), the  $\beta$ -barrel core is relatively static whereas the loops and helices framing the two binding sites show particular mobility. The presence of VP16(438-454) significantly alters the extent of

motion (Figure 2.9B). Particularly notable is that the upper loop on the H1 binding surface (residues 409-424 of Med25) appears to strongly interact with VP16. Supporting this model is the effect of mutations within this region on another H1-binding activator, ERM; a K411E mutation, for example, resulted in 4-fold weaker ERM binding (Fig. 2.3). The loop at the lower portion of this binding interface (residues 435-446) is also significantly altered upon interaction with VP16 and, again, interaction with H1 face-targeting ligands such as ERM is altered upon mutation at this site. The helices flanking the H1 binding surface also undergo significant stabilization upon binding, suggesting that they also play an important role in the defining the binding site. An analysis of RMSDs of residues in Med25-AcID unbound to any ligand reveals that the most dynamical regions of the protein are indeed the loops, with significant motion in the flanking helices as well, consistent with the preliminary structural model. Taken together, this model serves as a framework for targeting AcID's loop regions for small molecule discovery, the focus of Chapter 3.

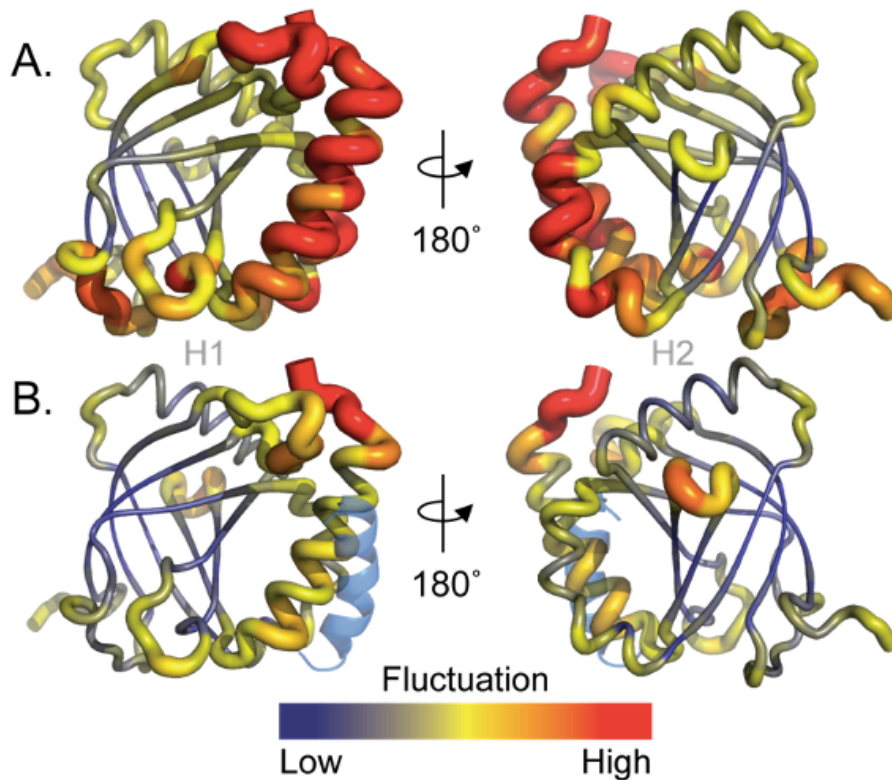


**Figure 2.9** Med25-Activator interaction binding model. (A,B) The NMR coordinates for Med25 AcID (PDB 2XNF) were used to construct the initial structure of Med25 in CHARMM using the Multiscale Modeling Tools for Structural Biology (MMTSB). For (B) VP16(438-454) G450C was constructed in CHARMM as a helical peptide<sup>23</sup>, which was then patched in CHARMM to Med25 C506 through the formation of a disulfide bond at C506 (transparent blue helix). Using GBSW implicit solvent<sup>2</sup>, temperature replica exchange was implemented using the CHARMM22 force field<sup>12</sup>. The root mean square fluctuations (RMSF) were calculated for each Med25-AcID residue by overlaying Ca atoms for all of the coordinate files produced from the simulations.<sup>17</sup> In this representation, the coloring correlates with the degree of dynamical behavior of each region. MD simulations done by Amanda Peiffer.

## 2.5 Materials and Methods

### Plasmids

The plasmid pET21b was used to produce the apo Med25(394-543) with a six histidine tag. This plasmid was received from Patrick Cramer as a gift.

## Protein Expression and Purification

Med25-AcID protein was transformed into BL21-AI competent cells. Ampicillin and streptomycin LB Agar plates were streaked and incubated at 37°C overnight. The next day, a 50 mL Terrific Broth (TB) starter culture with 5 $\mu$ L ampicillin (100mg/ml) and streptomycin (50mg/ml) was grown overnight with a picked colony from the LB plate at 37°C as well. The next morning, 7mL were used to inoculate the 1 liter TB that contained ampicillin and streptomycin. The bacteria was grown at 37°C to an OD<sub>600</sub> of 0.8. Once optimal OD<sub>600</sub> was achieved, 10% arabinose and IPTG was added and incubated at 27°C at 250 rpm overnight. The 1 liter TB culture was spun down to pellet using the floor centrifuge at 5000 rpm for 20 minutes at 4°C. Cell pellets were stored at -80°C. Cell pellet was resuspended in lysis buffer (components),  $\beta$ -mercaptoethanol, and an EDTA-free protease inhibitor tablet. The suspended cells were sonicated and filtered before purification. Sample was purified by FPLC with both Nickel (HisTrap, Buffer A: 50mM sodium phosphate, 300mM NaCl, and 30mM imidazole, pH 6.8 ; Buffer B: 50mM sodium phosphate, 300mM NaCl, and 400mM imidazole, pH 6.8) and Ion Exchange columns (Buffer A: 50mM sodium phosphate, 1mM DTT, pH 6.8 ; Buffer B: 50mM sodium phosphate, 1mM DTT, 1M NaCl, pH 6.8 ). Purified samples were collected and dialyzed in 10 mM sodium phosphate and 100 mM sodium chloride. The concentration of the resulting Med25 was measured using a Nanodrop at wavelength 280 nm using the extinction coefficient  $\epsilon=22460 \text{ M}^{-1}\text{cm}^{-1}$ .

## Peptide Synthesis

Peptides were synthesized on Rink amide resin using standard Fmoc solid-phase synthesis methods on a Liberty Blue Microwave Synthesizer (CEM). Fmoc deprotections were completed by suspending the resin in 20% piperidine (ChemImpex) in DMF supplemented with 0.2 M Oxyma Pure (CEM) and irradiating under variable power to maintain a temperature of 90 °C for 60 seconds. Coupling reactions were completed by combining the amino acid (5 eq relative to resin; CEM, ChemImpex, and NovaBiochem), diisopropylcarbodiimide (7 eq, ChemImpex), and Oxyma Pure (5 eq) in DMF and irradiating under variable power to maintain a temperature of 90 °C for 4 minutes. The resin was rinsed four times with an excess of DMF between all deprotection and coupling steps.

After synthesizing, resin was coupled with a fluorescein isothiocyanate (FITC) tag. 95%TFA / 2.5%TIPPS / 2.5% water cocktail solution was used to cleave from resin for 3 hours. Diethyl ether precipitation was used following resin cleavage. Peptides were purified using reverse-phase HPLC (Agilent) in 100mM ammonium acetate and acetonitrile as the organic phase. Purified fractions were collected, lyophilized then reconstituted in DMSO. Peptide concentration was obtained by UV-Vis spectrometer where samples were prepared in 6M guanidinium chloride with a 1:1000 ratio.

Peptides were synthesized with N-terminal  $\beta$ -alanine ( $\beta$ -Ala) and FITC tagged to the following sequences. HPLC purification was done over a 10-50% gradient in acetonitrile and 100 mM ammonium acetate solvent system. Correct peptides were identified through mass spectrometry efforts with the use of Agilent Q-ToF analysis.

	<b>Sequences</b>
Erm <sub>38-72</sub>	FITC β-Ala DLAHDSEELFQDLSQLQEAWLAEAQVPDDEQFVPD
Erm <sub>38-68</sub>	FITC β-Ala DLAHDSEELFQDLSQLQEAWLAEAQVPDDEQ
ATF6 $\alpha_{40-66}$	FITC βAla DTDELQLEAANETYENNFDNLDFDL
VP16 $\alpha$ H2 <sub>467-488</sub>	FITC βAla ALDMADFEFEQMFTDALGIDEY

	<b>Primers</b>
R466D Forward	CTGGACCATCCTTGAGTTATCGAACAAAGGGCCCAG
R466D Reverse	CTGGGCCCTTTGTTCGATAACTCAAGGATGGTCCAG
K411E Forward	CTGGAGTGGCAAGAGGAGCCCAAACCTGCCTCA
K411E Reverse	TGAGGCAGGTTTGGGCTCCTCTTGCCACTCCAG
R538E Forward	GGCTTCGTCAACGGCATCGAACAGGTCATCACCAACCTC
R538E Reverse	GAGGTTGGTGATGACCTGTTTCGATGCCGTTGACGAAGCC
Q451E Forward	CCAGAAGCTGATCATGGAACCTCATCCCCCAGCAG
Q451E Reverse	CTGCTGGGGGATGAGTTCCATGATCAGCTTCTGG
M523E Forward	AAGAAGAAGATCTTCGAAGGCCTCATCCCCTA
M523E Reverse	TAGGGGATGAGGCCTTCGAAGATCTTCTTCTT

### Direct Binding Experiments

Direct binding experiments were measured with fluorescence polarization and performed in black 384-well plates (Corning) and read using the PHERAStar multi-mode plate reader. The fluorescein isothiocyanate (FITC) labeled peptide was diluted to a stock concentration of 50 nM. Med25 concentration was diluted by half for the indicated data

points. Each well contained a final volume of 20 $\mu$ L with a final concentration of 25 nM. The data obtain was analyzed using GraphPad Prism software's nonlinear regression using the One Site Total Binding equation.

$$Y=Bmax*X/(Kd+X) + NS*X + Background$$

### Modeling Experimental

The objectives of our modeling efforts were to predict an ensemble of putative structures for the N-terminal predicted helical fragment of VP16(438-454) G450C tethered to the Med25 AcID domain C506 via a disulfide Tether. Our modeling was initiated from the published NMR coordinates for Med25 AcID (PDB) 2xnf). The protein structure of Med25 AcID was prepared for simulation in CHARMM using the Multiscale Modeling Tools for Structural Biology (MMTSB). VP16 has been shown to form a helical conformation when in complex with Med25 AcID, so VP16(438-454) G450C was constructed in CHARMM as contiguous helix, which was then patched using DISU patch in CHARMM to Med25 C506 through the formation of a disulfide bond. Prior to running the implicit solvent simulations, Med25 was fixed using harmonic restraints, and the complex was minimized with 1000 steps of a steepest descent algorithm. Using GBSW implicit solvent, temperature replica exchange was implemented using the CHARMM22 force field. These simulations were run for a total of 60 ns (2 fs time steps) using 12 replicas, sampling between 280-500 K and attempting coordinate exchanges every 5000 steps. The 12 replica trajectories were sorted by their respective temperatures, and the last 40 ns of the 280 K trajectories were then parsed into 4000 coordinate files. The MMTSB tool cluster.pl was used to cluster these structures, using K-means clustering with 1.5 Å RMSD cutoff for the superposed

C $\alpha$  backbone atoms for all the structures. The root-mean-square fluctuations (RMSF) for the last 40 ns of the 280 K trajectory were calculated for each Med25 AcID residue by superposing C $\alpha$  atoms of the coordinate files produced from the simulations. Clustering of the 4000 structures from the trajectories resulted in 20 clusters for apo Med25 AcID, with the highest populated cluster containing 40% of the structures; the Med25 AcID VP16(438-454) G450C complex resulted in 5 clusters, with the highest populated cluster containing 72% of the 4000 structures.

## 2.6 References

1. Bontems, François, et al. "NMR Structure of the Human Mediator MED25 ACID Domain." *Journal of Structural Biology*, vol. 174, no. 1, 2011, pp. 245–51, doi:<https://doi.org/10.1016/j.jsb.2010.10.011>.
2. Chen, Jianhan, et al. "Balancing Solvation and Intramolecular Interactions: Toward a Consistent Generalized Born Force Field." *Journal of the American Chemical Society*, vol. 128, no. 11, American Chemical Society, Mar. 2006, pp. 3728–36, doi:10.1021/ja057216r.
3. Dames, Sonja A., et al. "Structural Basis for Hif-1 $\alpha$ /CBP Recognition in the Cellular Hypoxic Response." *Proceedings of the National Academy of Sciences*, vol. 99, no. 8, Apr. 2002, p. 5271, doi:10.1073/pnas.082121399.
4. De Guzman, Roberto N., et al. "Interaction of the TAZ1 Domain of the CREB-Binding Protein with the Activation Domain of CITED2: REGULATION BY COMPETITION BETWEEN INTRINSICALLY UNSTRUCTURED LIGANDS FOR NON-IDENTICAL BINDING SITES." *Journal of Biological Chemistry*, vol. 279, no. 4, Jan. 2004, pp. 3042–49, doi:10.1074/jbc.M310348200.



5. de Launoit, Yvan, et al. "The Ets Transcription Factors of the PEA3 Group: Transcriptional Regulators in Metastasis." *Biochimica et Biophysica Acta (BBA) - Reviews on Cancer*, vol. 1766, no. 1, Aug. 2006, pp. 79–87, doi:10.1016/j.bbcan.2006.02.002.
6. Dyson, H. Jane, and Peter E. Wright. "Role of Intrinsic Protein Disorder in the Function and Interactions of the Transcriptional Coactivators CREB-Binding Protein (CBP) and P300." *Journal of Biological Chemistry*, vol. 291, no. 13, Mar. 2016, pp. 6714–22, doi:10.1074/jbc.R115.692020.
7. El Khattabi, Laila, et al. "A Pliable Mediator Acts as a Functional Rather Than an Architectural Bridge between Promoters and Enhancers." *Cell*, vol. 178, no. 5, Aug. 2019, pp. 1145-1158.e20, doi:10.1016/j.cell.2019.07.011.
8. Henderson, Andrew R., et al. "Conservation of Coactivator Engagement Mechanism Enables Small-Molecule Allosteric Modulators." *Proceedings of the National Academy of Sciences*, vol. 115, no. 36, Sept. 2018, p. 8960, doi:10.1073/pnas.1806202115.
9. Ikeda, Keiko, et al. "The H1 and H2 Regions of the Activation Domain of Herpes Simplex Virion Protein 16 Stimulate Transcription through Distinct Molecular Mechanisms." *Genes to Cells*, vol. 7, no. 1, John Wiley & Sons, Ltd, Jan. 2002, pp. 49–58, doi:10.1046/j.1356-9597.2001.00492.x.
10. Jifeng Zhang ED1 - Weibo Cai ED2 - Hao Hong. "Protein-Protein Interactions in Salt Solutions." *Protein-Protein Interactions*, IntechOpen, 2012, p. Ch. 18, doi:10.5772/38056.

11. Landrieu, Isabelle, et al. "Characterization of ERM Transactivation Domain Binding to the ACID/PTOV Domain of the Mediator Subunit MED25." *Nucleic Acids Research*, vol. 43, no. 14, Aug. 2015, pp. 7110–21, doi:10.1093/nar/gkv650.
12. MacKerell, A. D., et al. "All-Atom Empirical Potential for Molecular Modeling and Dynamics Studies of Proteins." *The Journal of Physical Chemistry B*, vol. 102, no. 18, American Chemical Society, Apr. 1998, pp. 3586–616, doi:10.1021/jp973084f.
13. Mapp, Anna K., et al. "Targeting Transcription Is No Longer a Quixotic Quest." *Nature Chemical Biology*, vol. 11, no. 12, Dec. 2015, pp. 891–94, doi:10.1038/nchembio.1962.
14. Milbradt, Alexander G., et al. "Structure of the VP16 Transactivator Target in the Mediator." *Nature Structural & Molecular Biology*, vol. 18, no. 4, Apr. 2011, pp. 410–15, doi:10.1038/nsmb.1999.
15. Okur, Halil I., et al. "Beyond the Hofmeister Series: Ion-Specific Effects on Proteins and Their Biological Functions." *The Journal of Physical Chemistry B*, vol. 121, no. 9, American Chemical Society, Mar. 2017, pp. 1997–2014, doi:10.1021/acs.jpccb.6b10797.
16. Perez-Jimenez, Raul, et al. "The Efficiency of Different Salts to Screen Charge Interactions in Proteins: A Hofmeister Effect?" *Biophysical Journal*, vol. 86, no. 4, Apr. 2004, pp. 2414–29, doi:10.1016/S0006-3495(04)74298-8.
17. Schrank, Travis P., et al. "Rational Modulation of Conformational Fluctuations in Adenylate Kinase Reveals a Local Unfolding Mechanism for Allostery and Functional Adaptation in Proteins." *Proceedings of the National Academy of Sciences*, vol. 106, no. 40, Oct. 2009, p. 16984, doi:10.1073/pnas.0906510106.

18. Sela, Dotan, et al. "Role for Human Mediator Subunit MED25 in Recruitment of Mediator to Promoters by Endoplasmic Reticulum Stress-Responsive Transcription Factor ATF6 $\alpha$ ." *Journal of Biological Chemistry*, vol. 288, no. 36, Sept. 2013, pp. 26179–87, doi:10.1074/jbc.M113.496968.
19. Shamma, Sarah L., Michael D. Crabtree, et al. "Insights into Coupled Folding and Binding Mechanisms from Kinetic Studies." *Journal of Biological Chemistry*, vol. 291, no. 13, Mar. 2016, pp. 6689–95, doi:10.1074/jbc.R115.692715.
20. Shamma, Sarah L., Alexandra J. Travis, et al. "Remarkably Fast Coupled Folding and Binding of the Intrinsically Disordered Transactivation Domain of CMYb to CBP KIX." *The Journal of Physical Chemistry B*, vol. 117, no. 42, American Chemical Society, Oct. 2013, pp. 13346–56, doi:10.1021/jp404267e.
21. Sheinerman, Felix B., et al. "Electrostatic Aspects of Protein–Protein Interactions." *Current Opinion in Structural Biology*, vol. 10, no. 2, Apr. 2000, pp. 153–59, doi:10.1016/S0959-440X(00)00065-8.
22. Sugita, Yuji, and Yuko Okamoto. "Replica-Exchange Molecular Dynamics Method for Protein Folding." *Chemical Physics Letters*, vol. 314, no. 1, Nov. 1999, pp. 141–51, doi:10.1016/S0009-2614(99)01123-9.
23. Uesugi, Motonari, et al. "Induced  $\alpha$  Helix in the VP16 Activation Domain upon Binding to a Human TAF." *Science*, vol. 277, no. 5330, Aug. 1997, p. 1310, doi:10.1126/science.277.5330.1310.
24. Uversky, Vladimir N., et al. "Intrinsically Disordered Proteins in Human Diseases: Introducing the D2 Concept." *Annual Review of Biophysics*, vol. 37, no. 1, Annual

Reviews, May 2008, pp. 215–46,  
doi:10.1146/annurev.biophys.37.032807.125924.

25. Verger, Alexis, et al. “The Mediator Complex Subunit MED25 Is Targeted by the N-Terminal Transactivation Domain of the PEA3 Group Members.” *Nucleic Acids Research*, vol. 41, no. 9, May 2013, pp. 4847–59, doi:10.1093/nar/gkt199.
26. Vojnic, Erika, et al. “Structure and VP16 Binding of the Mediator Med25 Activator Interaction Domain.” *Nature Structural & Molecular Biology*, vol. 18, no. 4, Apr. 2011, pp. 404–09, doi:10.1038/nsmb.1997.
27. Wang, Yanming, and Charles L. Brooks III. “Electrostatic Forces Control the Negative Allosteric Regulation in a Disordered Protein Switch.” *The Journal of Physical Chemistry Letters*, vol. 11, no. 3, American Chemical Society, Feb. 2020, pp. 864–68, doi:10.1021/acs.jpcllett.9b03618.

## **Chapter 3.**

### **Using Covalent Fragment to Target a Key Dynamic Substructure in Med25**

#### **3.1 Abstract**

Covalent probes are advantageous to use against dynamic proteins because they are able to stabilize different conformations that could play a key role in recognition and in gene expression. The focus of Chapter 3 is the use of covalent fragments to target a dynamic substructure of Med25-AcID. These results build from the previously defined importance of the positively charged substructures of Med25-AcID for guiding activator binding. The data herein supports a model in which that covalently targeting the domain's loop regions can provide a framework for developing probes for this class of dynamic proteins. More specifically we demonstrate that disulfide Tethering methods successfully identify fragment probes that target Med25-AcID, stabilize its substructures, and enhance the binding of at least one transcriptional activator binding partners. Further, assessment of analogs of one fragment revealed that the loop comprising Cys506 likely forms a chiral surface that should be targeted by noncovalent small molecule ligands.

#### **3.2 Introduction**

Covalently Targeting Dynamic Proteins

The screening method of Tethering came about as a way of finding a good fragment starting point to develop drugs. This process is a more efficient means of searching a binding surface for good small molecule-binding subsites as it identifies weak affinity fragments at predetermined positions. This is a suitable approach for coactivator proteins because there is no pharmacophore framework for dynamic proteins and because the binding surfaces are typically ill-defined. Tethering relies on the reversible covalent bond formation between a disulfide-containing fragment molecule and a cysteine-containing protein. If there is sufficient affinity of the fragment molecule for the binding surface and the disulfide moiety is close enough to the cysteine to undergo an exchange reaction, a covalent bond will form. The resulting adduct can then be identified by mass spectrometry. Due to the presence of a reducing agent such as  $\beta$ -mercaptoethanol, the resulting spectra typically show three species: protein alone, protein + reductant, and protein + fragment. The most prevalent will be the protein + fragment species if the fragment has inherent affinity for the protein of interest.

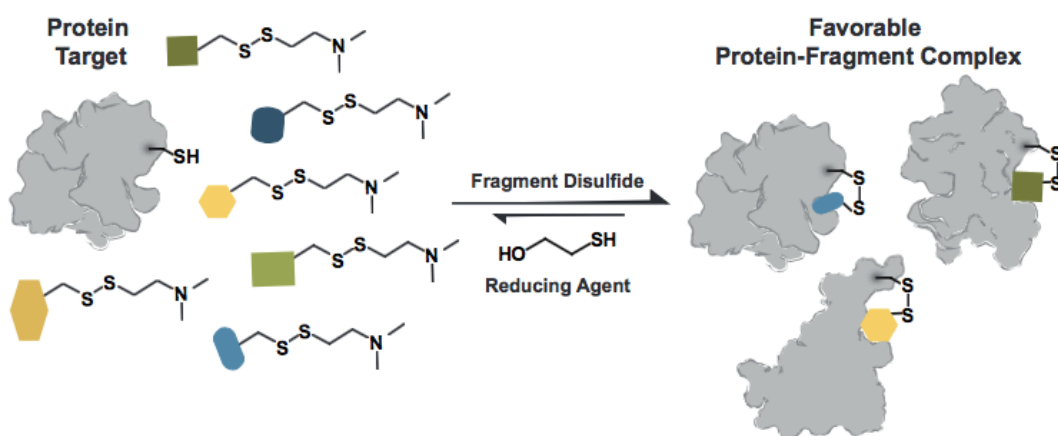


**Figure 3.1** Tethering Schematic. Cysteine containing protein target incubated with disulfide fragment forms protein-fragment complex with a covalent bond under reducing environment.

An example of the successful application of Tethering to dynamic coactivators is shown in previous work from the Mapp lab with a domain of the master coactivator CBP/p300. The CBP/p300 kinase-inducible domain (KIX) is structurally dynamic and has two binding surfaces as does Med25-AcID.<sup>11</sup> The transcriptional activators MLL and pKID form a ternary complex with KIX, with approximately two-fold enhancement of pKID affinity when MLL is prebound.<sup>18</sup> To investigate if a small-molecule could alter the allosteric network connecting the two binding sites, a Tethering screen was performed on four distinct cysteine mutants of KIX, each of which had a cysteine positioned in a distinct location around the MLL binding site (Figure 3.2A). From this screen the fragment 1-10 emerged as one of the leading candidates (Figure 3.2B). As shown in Figure 3.2C, 1-10 can enhance the affinity of pKID to KIX when the fragment is bound at the N627C site and inhibit 2-fold when bound at L664C. In other words, the binding site is malleable such that more than one binding pose can accommodate 1-10, each with a distinct functional outcome. Structural studies of the 1-10 complexes revealed that the flexible loop rimming the MLL binding surface plays the most significant role in this dynamic accommodation.

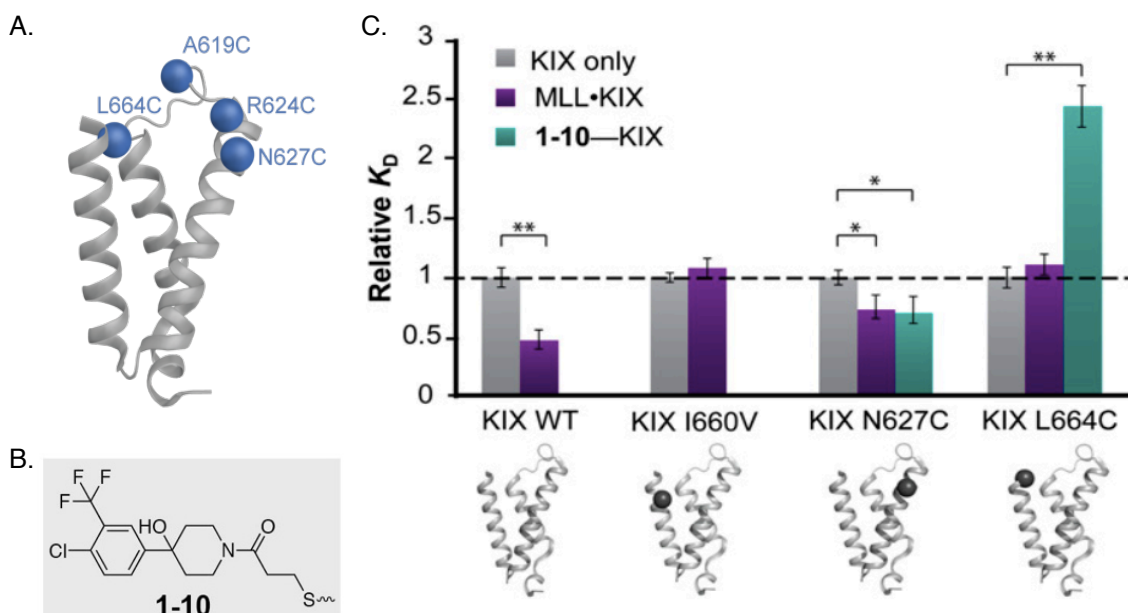


**Figure 3.2** Disulfide Fragment Targets KIX dynamic structure. (A) Cysteine mutations placed around the MLL binding site of the KIX domain and screened against a disulfide library. (B) Fragment 1-10 was isolated from the screen as lead fragment. (C) Fragment 1-10 when tethered to different positions in the MLL site changes the dissociation constant.

Despite having a considerably different structure than KIX, Med25-AcID is similarly dynamic, with both NMR structural studies and molecular dynamics simulations indicating regions of considerable disorder.<sup>19</sup> Further, the studies described in Chapter 2 support a model in which the most dynamic substructures – including flexible loops - within Med25-AcID play key roles in both molecular recognition and in allosteric communication between binding sites. Med25-AcID has three native cysteines, two of which are positioned near flexible loop regions. Cysteine 429, one of the least solvent exposed of the three, is angled pointing inside of the  $\beta$ -barrel. The remaining two cysteines are solvent exposed, one more than the other. Cysteine 497 is located on the H1 face of the

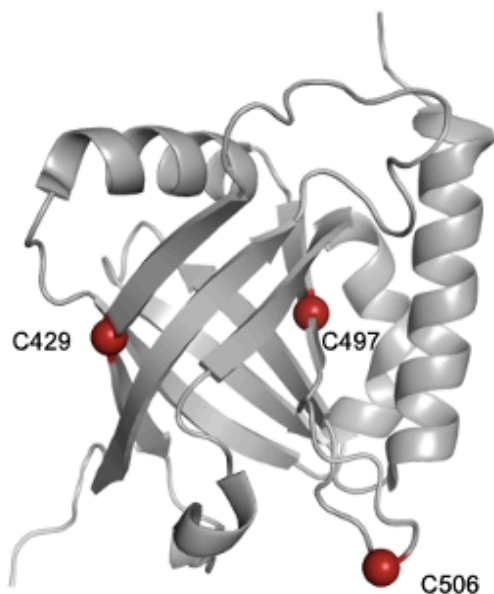


**Figure 3.3** Cartoon representation of Med25-AcID with the domain's native cysteine residues shown in red spheres.



domain pointing into solution and in close proximity to the top loop region and side helix substructure of the H1 face. Cysteine 506 is most accessible, located on the bottom loop region. A previous colleague in the Mapp lab, Dr. Andrew Henderson tested the reactivity of the cysteines through treatment with an excess of four different iodoacetamide-containing compounds followed by analysis by mass spectrometry. All four compounds have varying percentages of monolabeled species where percentage ranges from 10% (iodoacetic acid) to above 80% (iodoacetamide). Fragments 4-iodoacetamidosalicylic acid (IASalicylic acid), iodoacetamidodimethylbenzene (IAdimethylbenzene), and iodoacetamide also double label Med25-AcID. Mutational analysis revealed that cysteine 506 is the most reactive, cysteine 497 reacts with IASalicylic acid, and cysteine 429 showed no reactivity under these conditions, consistent with its lack of surface exposure in the structural model. With reactive cysteines positioned adjacent to and within dynamic loop regions, we thus hypothesized that disulfide Tethering could be an effective strategy to allosterically regulate Med25 binding and function.

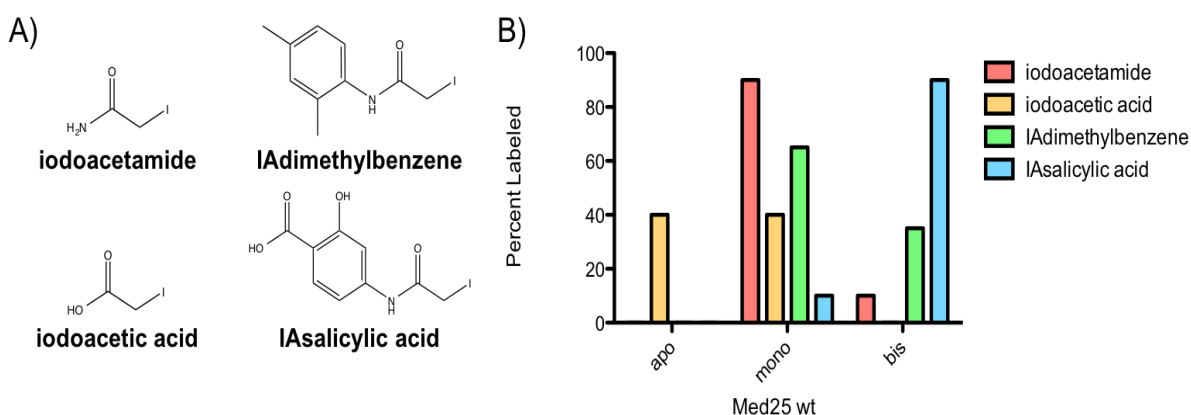


**Figure 3.4** Med25-AcID native cysteine accessibility. (A) Four covalent fragments with highly reactive electrophilic groups incubated with Med25. (B) Results from Tethering experiments identified by mass spectrometry show Med25-fragment species. Work carried out by Dr. Andrew Henderson.

### 3.3 Results and Discussion

#### Fragment Discovery in Med25 Using Disulfide Tethering

Wild-type Med25-AcID was screened against a 1600-member disulfide fragment library with the expectation that molecules that selectively label C497 or C506 would be identified, as well as have allosteric effects on activator binding.<sup>8</sup> This was carried out in collaboration with Dr. Jim Well's lab with postdoctoral fellow Dr. Zachary Hill at UCSF.<sup>4,5</sup> After expression of sufficient quantities of Med25-AcID and identifying appropriate buffer conditions for the screen, materials were transferred to UCSF. For the screen concentrations of Med25-AcID and fragments were held at 100  $\mu$ M while two concentrations of  $\beta$ -mercaptoethanol (BME) were used, 100  $\mu$ M and 1 mM.  $\beta$ -mercaptoethanol concentration was increased to report on the affinity of the Tethered species; fragments that remain bound even at 1 mM BME are higher affinity ligands than those that only bind with lower concentrations of BME. Molecules were considered hits that bound to Med25-AcID at levels greater than 3 standard deviations above the mean with BME concentrations at 100  $\mu$ M.

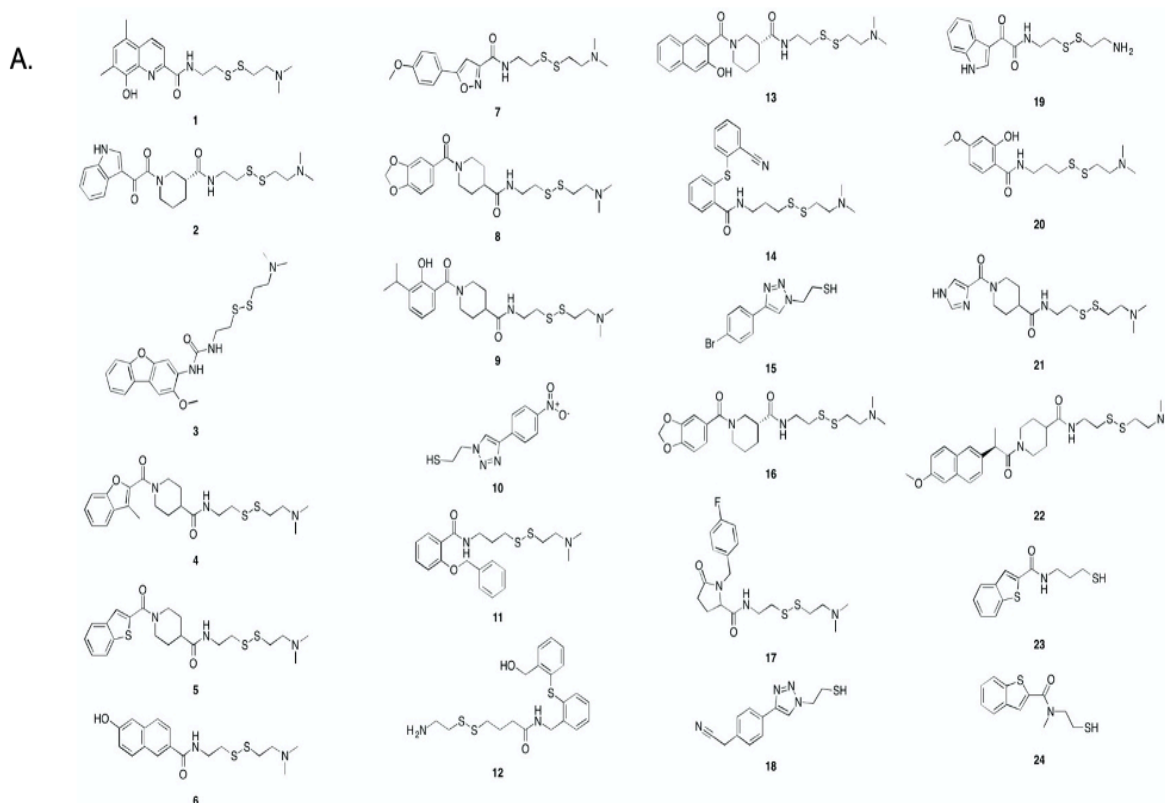
**Table 3.1** The Mass Spectrometry Tethering Screen Results

Compound #	Sample Name	Original Screen (100 $\mu$ M Fragment, 1 mM BME)				Follow-up (100 $\mu$ M Fragment, 100 $\mu$ M BME)			
		% 1xTethered	% 2xTethered	% 3xTethered	Total Tethered	% 1xTethered	% 2xTethered	% 3xTethered	Total Tethered
1	Med25 Plate 4 I16	48	18	4	70	35	21	2	58
2	Med25 Plate 2_B15	43	0	0	43	73	2	0	75
3	Med25 Plate 1 J19	39	9	1	49	45	13	5	63

4	Med25 Plate 4_P15	29	0	0	29	68	2	0	70
5	Med25 Plate 4_B22	23	0	0	23	74	1	0	75
6	Med25 Plate 4_F3	22	1	0	23	39	21	0	60
7	Med25 Plate 4_O12	22	9	2	33	24	18	14	56
8	Med25 Plate 2_K16	21	0	0	21	49	0	0	49
9	Med25 Plate 2_O14	21	0	0	21	41	0	0	41
10	Med25 Plate 5_D7	21	42	0	63	15	8	0	23
11	Med25 Plate 3_P7	20	0	0	20	59	3	0	62
12	Med25 Plate 1_O13	18	0	0	18	49	0	0	49
13	Med25 Plate 2_H11	18	0	0	18	49	1	0	50
14	Med25 Plate 2_I7	18	0	0	18	52	1	0	53
15	Med25 Plate 5_D9	18	8	2	28	23	10	5	38
16	Med25 Plate 2_J11	17	0	0	17	47	0	0	47
17	Med25 Plate 4_O10	17	0	0	17	46	0	0	46
18	Med25 Plate 5_H15	17	5	0	22	15	4	1	20
19	Med25 Plate 1_E15	16	1	0	17	40	11	0	51
20	Med25 Plate 1_P6	16	0	0	16	51	5	0	56
21	Med25 Plate 2_O16	16	1	0	17	32	1	1	34
22	Med25 Plate 4_H16	16	0	0	16	75	0	1	76
23	Med25 Plate 5_G9	16	1	0	17	47	16	0	63

24	Med25 Plate 5_E12	16	0	0	16	47	13	0	60
----	-------------------------	----	---	---	----	----	----	---	----

After identifying these hits, secondary screening efforts were carried out to identify which of the solvent exposed cysteines were being Tethered. To do this, the 24 hits were incubated with a Med25-AcID mutant where cysteine 506 was changed to an alanine residue. There was minimal tethering occurring at cysteine 497. Compounds such as 10 and 15 were among the higher tethering percentages which tethered at 20% and above more specific to cysteine 497. The low tethering percentages seen on the alanine mutant of cysteine 506 protein confirmed that cysteine 506 was being Tethered by the 24 hits.



B.

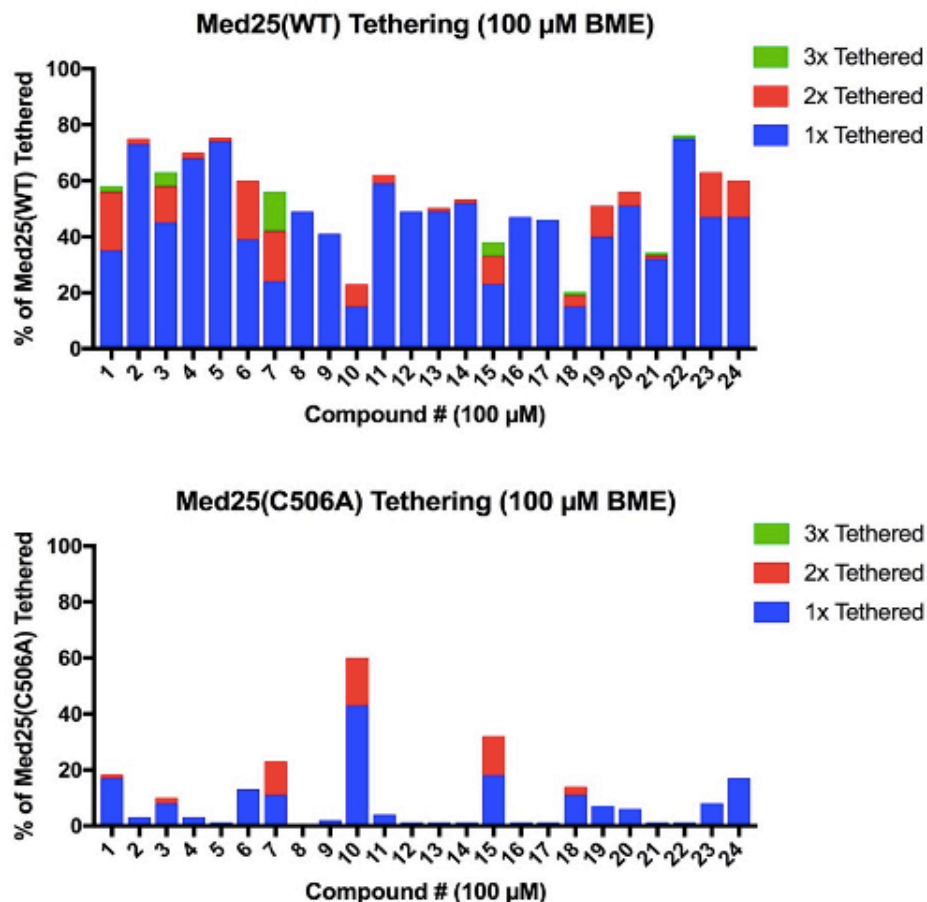
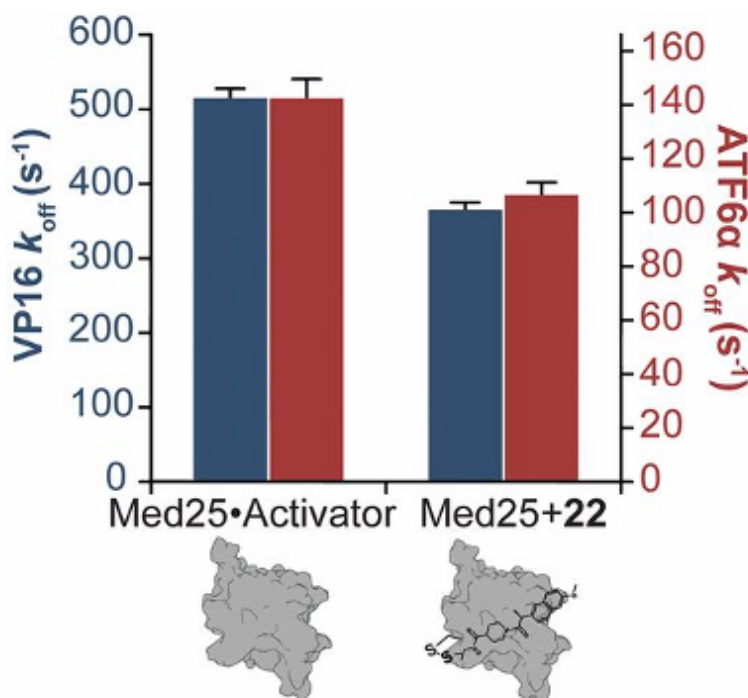


**Figure 3.5** Results of the tethering screen with wild-type Med25-AcID and C506C mutant. (A) The structure of the 24 hit fragments above 3 standard deviations are displayed. (B) This shows the percent tethering of the 24 hits with Med25 wild-type and mutant C506A. Screening experiments were carried out Dr. Zachary Hill.

Among the 24 fragments, several structures emerged as particularly interesting due to their high Tethering percentage (60%), compounds 2, 4, 5, 11, and 22. Among those compounds 2, 4, 11, and 22 showed high selectivity for C506. In particular, fragment 22 was found to tether at 75% and is specific to cysteine 506. There was then interest in understanding what structural features of the fragment allows for this high tethering percentage and selectivity for Cys506.

## Targeted Dynamic Substructure Allows for Allosteric Modulation

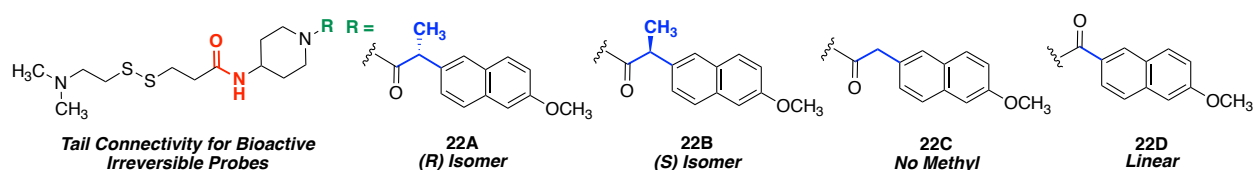
After identifying fragment 22, the allosteric effects of fragment 22 were tested by using transient kinetic experiments.<sup>17,14,12,10,2</sup> The control set of experiments worked where Med25-AcID was incubated with the fluorescently labeled DMN VP16 and an acetylated version was rapidly mixed in proper stopped-flow procedures.<sup>9,16</sup> The fluorescence read-out showed a  $k_{\text{off}}$  value of  $517 \text{ s}^{-1}$ . Med25-AcID was tethered to fragment 22 and this decreased the  $k_{\text{off}}$  value to  $367 \text{ s}^{-1}$ , an approximately 25% reduction. The same set of experiments were carried out using the activator ATF6 $\alpha$ .<sup>13</sup> The controlled experiment  $k_{\text{off}}$  value was  $143 \text{ s}^{-1}$  and protein-fragment complex is  $107 \text{ s}^{-1}$ . The observed  $k_{\text{off}}$  values show that there is an increase in the binding of both activators as a result of the fragment binding.



**Figure 3.6** Fragment 22 alters activator binding to Med25. The bar graph represents a comparison of  $k_{\text{off}}$  values of activators VP16 and ATF6 $\alpha$  with Med25-AcID with fragment 22 tethered and without the fragment present.

To probe this question, Dr. Brittany Morgan designed and synthesized derivatives of fragment 22 in which the connectivity between the carbonyl and the naphthyl moiety was altered. Interests were in this moiety due to its proximity to the naphthyl group and possible interactions with the pi system. Derivatives 22A and 22B addressed the sterics of the methyl group. In contrast, fragment 22C is removal of the methyl and 22D is the linear fragment with the removal of the central carbon that links the methyl group. This set of results shows that fragments 22 and 22A tether at similar single point tethering percentages under screening conditions. The fragments 22B, 22C, and 22D tether at lower single point tethering. Fragments 22A and 22B results show sterics of the fragments methyl group are important and suggests a chiral binding surface.

$\beta$ -Mercaptoethanol titration experiments were also used to rank the tethering efficiency of each derivative. The concentrations of Med25-AcID and disulfide fragment were held constant, while the  $\beta$ -Mercaptoethanol concentrations were varied. This data shows that it takes high concentrations of  $\beta$ -Mercaptoethanol to disassemble the 22 and 22A protein fragment complex. These Tethering events are more favorable events because of the presence and sterics of the methyl group. In contrast, compounds 22B, 22C, and 22D are bind more weakly than 22 and 22A.



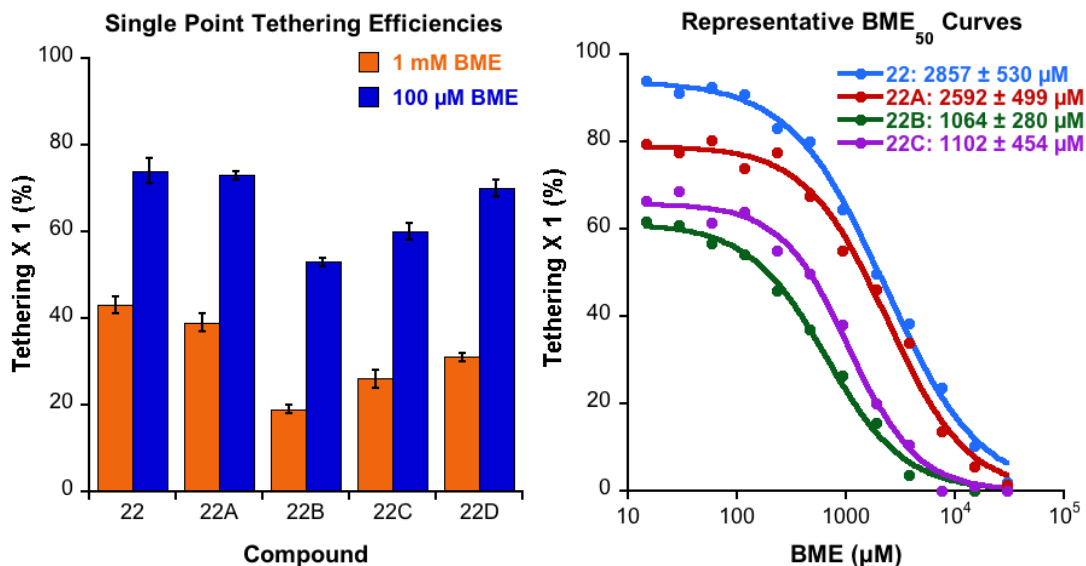
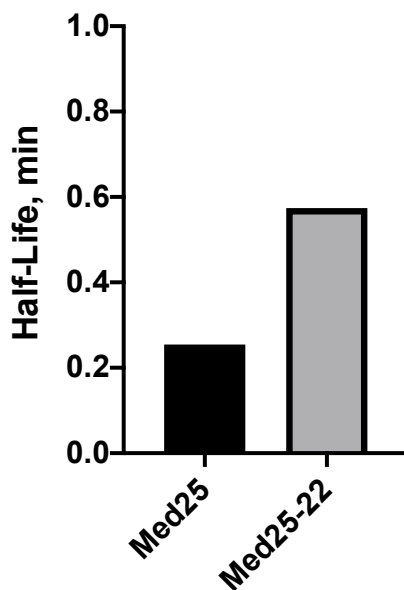


**Figure 3.7** Tethering efficiency of fragment 22 derivatives. (top row) Derivatives of fragment 22 were synthesized with changes to the methyl group. (Bottom row) Single point tethering and  $\beta$ -ME<sub>50</sub> curves were quantified by mass spectrometry. Experiments were done in collaboration with Dr. Brittany Morgan.

Med25-AcID is a coactivator that has dynamic substructures that allow it to interact with its binding partners. There have been examples in literature that contribute the changes seen in positive and negative cooperative binding to levels of stabilization within proteins.<sup>7</sup> The kinase-inducible domain (KIX) of the CBP coactivator complex is important in regulating transcriptional activity.<sup>3</sup> The KIX domain is able to be cooperatively targeted by transcription factors and small molecules.<sup>6</sup> There are significant changes this domain's stability that help alter activator binding when a small molecule is tethered.<sup>15</sup> Here is shown that Med25-AcID exhibits levels of stabilization when tethered to a small molecule fragment 22.



## Degradation Experiments



	<u>Half-Life, minutes</u>
Apo Med25	0.3 ± 0.1
Med25-22	0.6 ± 0.3

**Figure 3.8** Signs of Med25-AcID stabilization from fragment 22. This represents thermolysin degradation of apo Med25 and Med25 tethered to fragment 22.

### 3.4 Conclusions

Med25-AcID coactivator is a part of a difficult class of proteins to target in drug discovery. They are usually highly dynamic in nature and bind many different activators using limited binding sites. Taking from the findings in the previous chapter, this chapter used covalent probes to target the dynamic loop substructure of Med25-AcID. Through tethering screens, it identified a fragment that's selective to the native cysteine 506 that's located in the loop region. The fragment has the ability to covalently label one site and

communicate with the opposite binding surface.<sup>11</sup> This is seen through stopped-flow experiments where  $k_{\text{off}}$  values are decreased with activators ATF6 $\alpha$  and VP16. Degradation experiments were then carried out to determine there were levels of stabilization within the domain that participated in allow this event. Other efforts show there are components of the tethered fragment that help create for a successful tethering event. The stereochemistry of the methyl group proved to be essential through testing derivatives of the fragment. This also allowed us to draw conclusions about the tethered surface of Med25-AcID. It a chiral surface area that recognizes the fragment which is useful information in future development.

### **3.5 Materials and Methods**

#### Plasmids

The plasmid used to produce Med25(394-543) with a six histidine tag was pET21b. Patrick Cramer provided the plasmid.

#### Protein Expression and Purification

BL21-AI competent cells were used for transformation steps. Competent cells were resuspended and streaked across LB Agar plates containing streptomycin and ampicillin antibiotics. The plates were then incubated at 37°C overnight. A colony was picked and added to a 50 mL Terrific Broth (TB) starter culture which contained 5  $\mu\text{L}$  of ampicillin (100 mg/ml) and streptomycin (50 mg/ml). The next morning, 7mL were used to inoculate the 1 liter TB that contained ampicillin and streptomycin. The bacteria was grown at 37°C to an OD<sub>600</sub> of 0.8. Once optimal OD<sub>600</sub> was achieved, 10% arabinose and IPTG was

added and incubated at 27°C at 250 rpm overnight. The 1 liter TB culture was spun down to pellet using the floor centrifuge at 5000 rpm for 20 minutes at 4°C. Cell pellets were stored at -80°C. Cell pellet was resuspended in lysis buffer (components),  $\beta$ -Mercaptoethanol, and an EDTA-free protease inhibitor tablet. The suspended cells were sonicated and filtered before purification. Sample was purified by FPLC with both Nickel (HisTrap, Buffer A: 50 mM sodium phosphate, 300 mM NaCl, and 30 mM imidazole, pH 6.8 ; Buffer B: 50 mM sodium phosphate, 300 mM NaCl, and 400 mM imidazole, pH 6.8) and Ion Exchange columns (Buffer A: 50 mM sodium phosphate, 1 mM DTT, pH 6.8 ; Buffer B: 50 mM sodium phosphate, 1 mM DTT, 1 M NaCl, pH 6.8 ). Purified samples were collected and dialyzed in 10 mM sodium phosphate and 100 mM sodium chloride. The concentration of the resulting Med25 was measured using a Nanodrop at wavelength 280 nm using the extinction coefficient  $\epsilon=22460 \text{ M}^{-1}\text{cm}^{-1}$ .

#### Med25 labeling with disulfide fragments

The  $\beta$ -ME experiments were carried out at room temperature and quantified by Agilent Q-TOF HPLC-MS. Samples were injected on to a C<sub>8</sub> Poroshell column. There were data points collected over a range of 12  $\beta$ -ME data points ( 30, 15, 7.5, 3.8, 1.9, 0.94, 0.47, 0.23, 0.12, 0.059, 0.030, 0.015 mM ).

$$\text{Percent Tethered} = \frac{\text{Med25} - \text{fragment}}{(\text{apoMed25}) + (\text{Med25} - \text{fragment}) + (\text{Med25} - \beta\text{ME})}$$

#### Protein Degradation

Med25 wildtype and Med25-22 complex solutions were incubated at 60°C with the protease thermolysin.<sup>1</sup> Thermolysin cleaves proteins at the N-terminus of the hydrophobic

residues leucine, phenylalanine, isoleucine, alanine, and methionine. Solutions were diluted in proteolysis buffer ( 50 mM Tris-HCl, 100 mM NaCl, 0.5 mM CaCl<sub>2</sub>, and 4 M Urea ) with a final 1 to 4 molar ratio. The solutions were quenched with EDTA at a final concentration of 5 mM. Quantification was by ImageJ from Bis-Tris protein gel bands. Protein abundance values were recorded and fit to an exponential decay equation.

### 3.6 References

1. Agius, Michael P., et al. "Selective Proteolysis to Study the Global Conformation and Regulatory Mechanisms of C-Src Kinase." *ACS Chemical Biology*, vol. 14, no. 7, American Chemical Society, July 2019, pp. 1556–63, doi:10.1021/acscchembio.9b00306.
2. Dogan, Jakob, et al. "Fast Association and Slow Transitions in the Interaction between Two Intrinsically Disordered Protein Domains." *Journal of Biological Chemistry*, vol. 287, no. 41, Oct. 2012, pp. 34316–24, doi:10.1074/jbc.M112.399436.
3. Dyson, H. Jane, and Peter E. Wright. "Role of Intrinsic Protein Disorder in the Function and Interactions of the Transcriptional Coactivators CREB-Binding Protein (CBP) and P300." *Journal of Biological Chemistry*, vol. 291, no. 13, Mar. 2016, pp. 6714–22, doi:10.1074/jbc.R115.692020.
4. Erlanson, Daniel A., Andrew C. Braisted, et al. "Site-Directed Ligand Discovery." *Proceedings of the National Academy of Sciences*, vol. 97, no. 17, Aug. 2000, p. 9367, doi:10.1073/pnas.97.17.9367.
5. Erlanson, Daniel A., James A. Wells, et al. "Tethering: Fragment-Based Drug Discovery." *Annual Review of Biophysics and Biomolecular Structure*, vol. 33, no.

- 1, Annual Reviews, May 2004, pp. 199–223, doi:10.1146/annurev.biophys.33.110502.140409.
6. Gianni, Stefano, et al. “A Folding-after-Binding Mechanism Describes the Recognition between the Transactivation Domain of c-Myb and the KIX Domain of the CREB-Binding Protein.” *Biochemical and Biophysical Research Communications*, vol. 428, no. 2, Nov. 2012, pp. 205–09, doi:10.1016/j.bbrc.2012.09.112.
7. Guillory, Xavier, et al. “Fragment-Based Differential Targeting of PPI Stabilizer Interfaces.” *Journal of Medicinal Chemistry*, vol. 63, no. 13, American Chemical Society, July 2020, pp. 6694–707, doi:10.1021/acs.jmedchem.9b01942.
8. Henderson, Andrew R., et al. “Conservation of Coactivator Engagement Mechanism Enables Small-Molecule Allosteric Modulators.” *Proceedings of the National Academy of Sciences*, vol. 115, no. 36, Sept. 2018, p. 8960, doi:10.1073/pnas.1806202115.
9. Ikeda, Keiko, et al. “The H1 and H2 Regions of the Activation Domain of Herpes Simplex Virion Protein 16 Stimulate Transcription through Distinct Molecular Mechanisms.” *Genes to Cells*, vol. 7, no. 1, John Wiley & Sons, Ltd, Jan. 2002, pp. 49–58, doi:10.1046/j.1356-9597.2001.00492.x.
10. Johnson, Kenneth A. “[61] Rapid Kinetic Analysis of Mechanochemical Adenosinetriphosphatases.” *Structural and Contractile Proteins Part C: The Contractile Apparatus and the Cytoskeleton*, vol. 134, Academic Press, 1986, pp. 677–705, doi:10.1016/0076-6879(86)34129-6.

11. Sadowsky, Jack D., et al. "Turning a Protein Kinase on or off from a Single Allosteric Site via Disulfide Trapping." *Proceedings of the National Academy of Sciences*, vol. 108, no. 15, Apr. 2011, p. 6056, doi:10.1073/pnas.1102376108.
12. Schreiber, Gideon, and Alan R. Fersht. "Rapid, Electrostatically Assisted Association of Proteins." *Nature Structural Biology*, vol. 3, no. 5, May 1996, pp. 427–31, doi:10.1038/nsb0596-427.
13. Sela, Dotan, et al. "Role for Human Mediator Subunit MED25 in Recruitment of Mediator to Promoters by Endoplasmic Reticulum Stress-Responsive Transcription Factor ATF6 $\alpha$ ." *Journal of Biological Chemistry*, vol. 288, no. 36, Sept. 2013, pp. 26179–87, doi:10.1074/jbc.M113.496968.
14. Shammass, Sarah L., et al. "Insights into Coupled Folding and Binding Mechanisms from Kinetic Studies." *Journal of Biological Chemistry*, vol. 291, no. 13, Mar. 2016, pp. 6689–95, doi:10.1074/jbc.R115.692715.
15. Teilum, Kaare, et al. "Protein Stability, Flexibility and Function." *Protein Dynamics: Experimental and Computational Approaches*, vol. 1814, no. 8, Aug. 2011, pp. 969–76, doi:10.1016/j.bbapap.2010.11.005.
16. Vojnic, Erika, et al. "Structure and VP16 Binding of the Mediator Med25 Activator Interaction Domain." *Nature Structural & Molecular Biology*, vol. 18, no. 4, Apr. 2011, pp. 404–09, doi:10.1038/nsmb.1997.
17. Wands, Amberlyn M., et al. "Transient-State Kinetic Analysis of Transcriptional Activator-DNA Complexes Interacting with a Key Coactivator." *Journal of Biological Chemistry*, vol. 286, no. 18, May 2011, pp. 16238–45, doi:10.1074/jbc.M110.207589.

18. Wang, Ningkun, Jean M. Lodge, et al. "Dissecting Allosteric Effects of Activator–Coactivator Complexes Using a Covalent Small Molecule Ligand." *Proceedings of the National Academy of Sciences*, vol. 111, no. 33, Aug. 2014, p. 12061, doi:10.1073/pnas.1406033111.
19. Wang, Ningkun, Chinmay Y. Majmudar, et al. "Ordering a Dynamic Protein Via a Small-Molecule Stabilizer." *Journal of the American Chemical Society*, vol. 135, no. 9, American Chemical Society, Mar. 2013, pp. 3363–66, doi:10.1021/ja3122334.

## Chapter 4.

### Conclusions and Future Directions

#### 4.1 Conclusions of this work

The Mediator complex is an important portion of the pre-initiation complex that contains protein-protein interaction networks that are valuable therapeutic targets. The tail region of the Mediator complex is one of particular interest because of its association with transcription factors<sup>4</sup>. The transcription factors that associate with the tail module are involved in a number of diseases. In a key example that has been the focus of this work, the subunit Med25 participates in cancer metastasis through association with the Ets transcription factor Erm<sup>2</sup>. Like many protein-protein interactions, this interaction is thought to be “undruggable” due to difficulties of targeting the large and dynamic surface area of Med25<sup>11</sup>. There is thus a lack of therapeutic agents and probes that target coactivator Med25-AcID and others like it.

The work in this thesis was guided by the goal of identifying small molecule fragments that target the uniquely folded coactivator subunit Med25, in particular its activator binding motif AcID. The hypothesis was that the use of covalent fragments that target the dynamic substructure of Med25-AcID would inform a molecular recognition model for small-molecule targeting. This was based upon defining important principles of the coactivator-activator binding mechanism as shown in Chapter 2. We first determined



the important mechanistic features of the coactivator-activator interaction. Next, we carried out small molecule screens with a disulfide fragment library with Med25-AcID. Experiments were performed that identified the fragment's necessary characteristics for covalent labeling and effects on coactivator conformational dynamics.

As outlined in Chapter 2, work was done to define important mechanistic features of the Med25 coactivator-activator interaction. One such question was if activators bind to different binding surfaces in Med25-AcID, with a particular focus on the ETV/PEA3 activators, VP16, and ATF6 $\alpha$ <sup>14,16,17</sup>. We first determined where activators bind in the domain of Med25-AcID. Earlier HSQC NMR experiments were carried out with Erm and VP16, both H1 face binding activators. Mutagenesis within the AcID domain was guided by the shared perturbed residues of the Erm and VP16 HSQC NMR experiments. The resulting data revealed ATF6 $\alpha$  interacts on a different binding surface in contrast to Erm and VP16<sup>8</sup>. HSQC NMR experiments with the ATF6 $\alpha$  Med25-AcID complex further confirmed its interaction with the H2 face of the domain due to the perturbed residues found there. Thus, when planning small molecule targeting of Med25-AcID, there is a choice of binding sites to consider.

We were then interested in the electrostatic contacts of the interaction because Med25-AcID is positively charged and its activators are highly negative. This was particularly a line of inquiry because electrostatics was an essential component in a study done with the CBP Taz 1 domain and binding activators. It found that charge was very important in the ternary complex interactions with CITED2 and HIF-1 $\alpha$  transcriptional activation domains<sup>18</sup>. Insightful information of the Hoffmeister's series aided in designing the next set of experiments<sup>13,15</sup>. This series shows the ranking of ions based on their

strength to interact with proteins. Residue side chain interactions play a role in its ability to bind proteins along with other possible ion interacting mechanisms. Binding experiments with cations and anions of different strengths and concentrations show electrostatics are important in guiding activator interactions with Med25-AcID. Increasing the salt concentration in the assay buffer produces more ions that interrupt Med25-AcID activator binding events. Further experiments proved that the size of ions have varying effects on this PPI. The overall negative charge of activator Erm was decreased and further confirms this point on charge-charge contacts within the interface. From here we noticed that many of the positive residues were housed within the flexible substructures of the domain and molecular dynamic simulations showed these same regions stabilized upon binding activators<sup>8</sup>. The dynamic substructures were then considered for small-molecule targeting seeing the H1 face contains thiophilic handles available for covalent probes.

In Chapter 3, we carried out disulfide fragment screening methods<sup>5,6</sup>. Med25-AcID has three native cysteines within the domain. Of the three cysteines, two of them are solvent exposed and available for sufficient disulfide exchange. Cysteine 497 is placed in close proximity to the top loop region of the H1 face, while cysteine 506 is located on the bottom flexible loop region on the same surface. This could prove to be useful seeing these regions are important in activation domain binding. This was determined by experiments done by Dr. Andrew Henderson. He incubated Med25-AcID with small molecule fragments iodoacetamide, iodoacetamidosalicylic acid, iodoacetmidodimethylbenzene which all have a thiophilic leaving group. This set of mass spectrometry results showed Med25-AcID contained only single and double labeled

species present upon incubation. Further mutagenesis studies of cysteine 506 confirmed cysteines 506 and 497 are available for disulfide exchange. Screening was done in conjunction with the Dr. Jim Wells lab at the University of California San Francisco, where Dr. Zachery Hill was our collaborator. The disulfide Tethering method was used to identify hits with the use of mass spectrometry quantification. Experiments identified 24 hits that were above 3 standard deviations. We were interested in learning where the identified fragments labeled after identifying the hits from the initial screen. Building from the understanding Med25-AcID has two solvent exposed cysteines, both are located on the H1 face of the AcID domain. Cysteine 506 is located in the dynamic loop region and cysteine 497 is on the  $\beta$ -barrel. Expressed aliquots of wild-type Med25-AcID and cysteine 506 alanine (C506A) mutant were provided. Labeling of Med25-AcID drastically diminished with the mutant form of the protein. The two fragments that had moderated labeling which included fragments 10 & 15 which targeted cysteine 497.

Of the two screens, we were most interested in the fragment 22. This was of interest because of its ability to single tether at high percentages and specific to cysteine 506 located in the flexible loop substructure at the base of Med25 AcID. One of the advantages of using the Tethering method is that it can stabilize different conformations. This is a useful technique in targeting Med25-AcID because of the dynamic nature of the substructures found to be important for activator interaction. Experiments were then carried out to determine how fragment 22 alters binding of activator proteins. Stopped-flow kinetics was used to quantify the  $k_{off}$  values of the binding activators VP16 and ATF6 $\alpha$ . Results showed that fragment 22 decreases the  $k_{off}$  value of VP16 and ATF6 $\alpha$  activators<sup>8</sup>. This also shows that tethering the flexible loop region on the H1 face with

fragment 22 is able to change binding at the H2 face of Med25-AcID which is located on the opposite surface. Interest was then taken in understanding if the AcID domain was more stable in the presence of fragment 22. Apo AcID and AcID-22 complex were incubated with thermolysin protease. These results show there is moderate stabilization within the domain when fragment 22 is tethered to the flexible loop region. We then investigated which features of fragment 22 were essential for causing a successful tethering event. Derivatives of the fragment were made by Dr. Brittany Morgan that made changes to an important methyl group. Single-Point tethering experiments showed the presence and stereochemistry of the methyl group allowed for successful labeling of the protein.

Some of the major findings of this work conclude that the dynamic loop substructures of the coactivator Med25-AcID are an essential portion of binding its' associated activation domains. The charged residues of these regions guide interaction with a variety of activator proteins. The broader importance of learning the contributions of electrostatics has been seen in other coactivator-activator systems. Interactions that involve the coactivators Taz 1 and IBiD show examples and make suggestions that charge-charge interactions play critical roles in guiding activator binding. Work here also shows covalently targeting this region is advantageous because these probes can stabilize different conformations that can be effective in coactivator ternary complexes. Taken together this can serve as model to target dynamic substructures of coactivator proteins.

## **4.2 Future Directions**

## Electrostatic Selectivity Section

As talked about in detail in Chapter 2, electrostatics are an important component for guiding activators binding to Med25-AcID. The study done with the Taz1 domain in both binary and ternary complexes gives insight that determined electrostatic forces are essential for displacement of HIF-1 $\alpha$  by CITED2. This is interesting because it gives insight to what allows inhibitory effects that can be transferred principles in other coactivators and small molecule efforts. Taking this into account, this raises the broader question of how selectivity is achieved among activator-coactivator interactions. Coactivator proteins usually have designated domains that bind a variety of activator proteins on limited surfaces. In the coactivator class of proteins, surfaces vary in overall charge. Future experiments will include synthesizing control and experimental activator peptides that bind Med25-AcID. Experimental peptides will have negative charge residues mutated to polar residues that are close in size. For example, glutamic acid (Glu) will be changed to glutamine (Gln), and aspartic acid (Asp) will be changed to asparagine (Asn). The following changes in to the activator would be thought to effect selectivity of peptides to other coactivator domains. The same control and experimental peptides will be used to bind other coactivator domains such as the IBiD and KIX domains which are a part of the CBP coactivator complex<sup>3</sup>.

## Further Disulfide Fragment Assessment

The Tethering screen conducted and described in Chapter 3 identified fragment 22 as an enhancer of ATF6 $\alpha$  binding to Med25. It was identified as being specific in Tethering native cysteine 506 located in one of the domain's dynamic loop regions. This has the

ability to alter the  $k_{\text{off}}$  values of activators VP16 and ATF6 $\alpha$ . There is room for further quantification of the effects of the fragment on activator binding. This would include using Med25-AcID fragment complex and fluorescently labeled activator peptides to conduct fluorescence polarization assays. Binding affinities will be calculated where we would expect to see signs of increased. This would be expected because there have been previous studies on the CBP KIX domain that suggest stabilization of the domain can cause this type of change increased affinity.

In addition, the cell has a highly reducing environment. The fragment 22 currently exists in the reversible form which can easily be reduced. Fragment 22 would need to be converted to an irreversible form for engaging its' target in cells<sup>7,9</sup>. There are an array of electrophilic leaving groups that can be used. Electrophilic groups vary in reactivity and selectivity. For example, electrophiles such as chloroacetamide and bromodihydroisoxazoles are usually specific to cysteine residues where chloroacetamide is more reactive (electrophilic) than bromodihydroisoxazoles.

There were other interesting fragments identified from the screen that specifically targeted cysteine 497. Fragment 10 tethered at 15% to apo Med25-AcID. The same fragment labeled the cysteine 506 alanine mutant at higher percentages. This could be done as a comparative study on the effects of binding when targeting different substructure types.

Upon converting fragment 22 from a reversible to an irreversible form, the genes associated with Med25-activator protein-protein interactions. There is an association of HSP5 $\alpha$  gene with the activator ATF6 $\alpha$ , while the matrix-metalloprotease 3 with Erm<sup>1,16</sup>.

There can also be qPCR experiments that monitor expression levels of Erm and ATF6 $\alpha$  genes when cells are dosed with optimized irreversible 22 molecules.

### 4.3 References

1. Baert, Jean-Luc, et al. "Expression of the PEA3 Group of ETS-Related Transcription Factors in Human Breast-Cancer Cells." *International Journal of Cancer*, vol. 70, no. 5, 1997, pp. 590–97, doi:10.1002/(SICI)1097-0215(19970304)70:5<590::AID-IJC17>3.0.CO;2-H.
2. de Launoit, Yvan, et al. "The Ets Transcription Factors of the PEA3 Group: Transcriptional Regulators in Metastasis." *Biochimica et Biophysica Acta (BBA) - Reviews on Cancer*, vol. 1766, no. 1, Aug. 2006, pp. 79–87, doi:10.1016/j.bbcan.2006.02.002.
3. Dyson, H. Jane, and Peter E. Wright. "Role of Intrinsic Protein Disorder in the Function and Interactions of the Transcriptional Coactivators CREB-Binding Protein (CBP) and P300." *Journal of Biological Chemistry*, vol. 291, no. 13, Mar. 2016, pp. 6714–22, doi:10.1074/jbc.R115.692020.
4. El Khattabi, Laila, et al. "A Pliable Mediator Acts as a Functional Rather Than an Architectural Bridge between Promoters and Enhancers." *Cell*, vol. 178, no. 5, Elsevier, Aug. 2019, pp. 1145-1158.e20, doi:10.1016/j.cell.2019.07.011.
5. Erlanson, Daniel A., Andrew C. Braisted, et al. "Site-Directed Ligand Discovery." *Proceedings of the National Academy of Sciences*, vol. 97, no. 17, Aug. 2000, p. 9367, doi:10.1073/pnas.97.17.9367.

6. Erlanson, Daniel A., James A. Wells, et al. "Tethering: Fragment-Based Drug Discovery." *Annual Review of Biophysics and Biomolecular Structure*, vol. 33, no. 1, Annual Reviews, May 2004, pp. 199–223, doi:10.1146/annurev.biophys.33.110502.140409.
7. González-Bello, Concepción. "Designing Irreversible Inhibitors—Worth the Effort?" *ChemMedChem*, vol. 11, no. 1, John Wiley & Sons, Ltd, Jan. 2016, pp. 22–30, doi:10.1002/cmdc.201500469.
8. Henderson, Andrew R., et al. "Conservation of Coactivator Engagement Mechanism Enables Small-Molecule Allosteric Modulators." *Proceedings of the National Academy of Sciences*, vol. 115, no. 36, Sept. 2018, p. 8960, doi:10.1073/pnas.1806202115.
9. Jöst, Christian, et al. "Promiscuity and Selectivity in Covalent Enzyme Inhibition: A Systematic Study of Electrophilic Fragments." *Journal of Medicinal Chemistry*, vol. 57, no. 18, American Chemical Society, Sept. 2014, pp. 7590–99, doi:10.1021/jm5006918.
10. Landrieu, Isabelle, et al. "Characterization of ERM Transactivation Domain Binding to the ACID/PTOV Domain of the Mediator Subunit MED25." *Nucleic Acids Research*, vol. 43, no. 14, Aug. 2015, pp. 7110–21, doi:10.1093/nar/gkv650.
11. Mapp, Anna K., et al. "Targeting Transcription Is No Longer a Quixotic Quest." *Nature Chemical Biology*, vol. 11, no. 12, Dec. 2015, pp. 891–94, doi:10.1038/nchembio.1962.

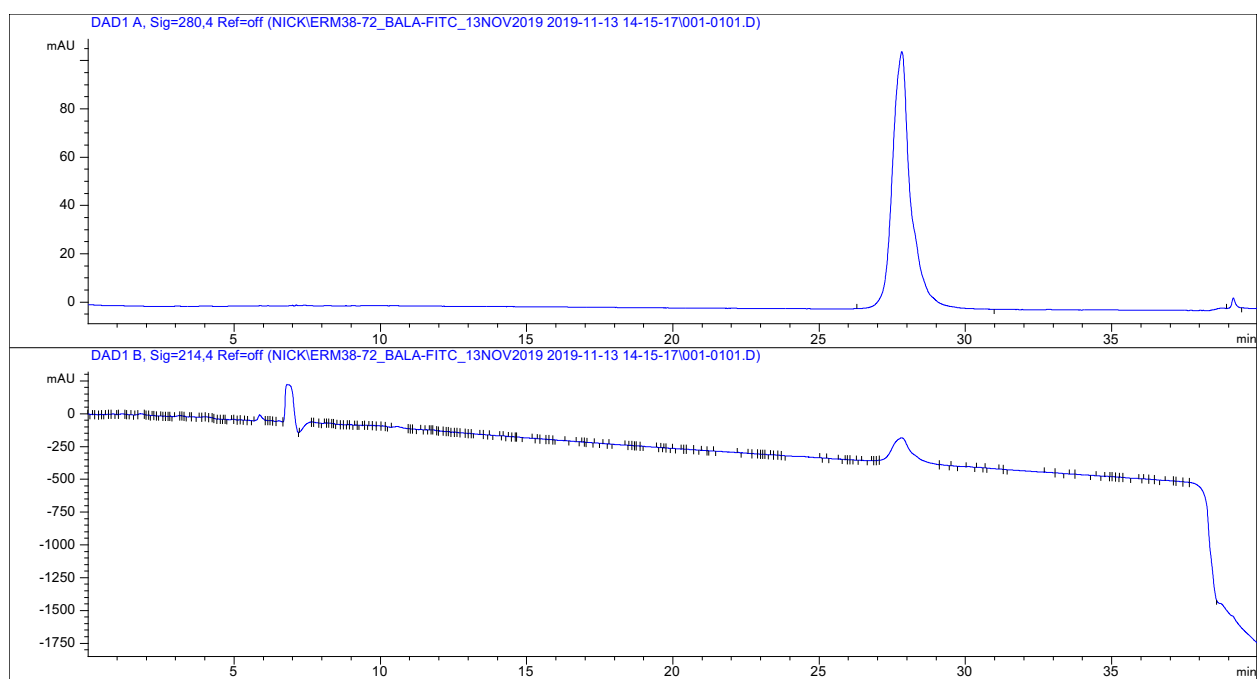


12. Milbradt, Alexander G., et al. "Structure of the VP16 Transactivator Target in the Mediator." *Nature Structural & Molecular Biology*, vol. 18, no. 4, Apr. 2011, pp. 410–15, doi:10.1038/nsmb.1999.
13. Okur, Halil I., et al. "Beyond the Hofmeister Series: Ion-Specific Effects on Proteins and Their Biological Functions." *The Journal of Physical Chemistry B*, vol. 121, no. 9, American Chemical Society, Mar. 2017, pp. 1997–2014, doi:10.1021/acs.jpcc.6b10797.
14. Sela, Dotan, et al. "Role for Human Mediator Subunit MED25 in Recruitment of Mediator to Promoters by Endoplasmic Reticulum Stress-Responsive Transcription Factor ATF6 $\alpha$ ." *Journal of Biological Chemistry*, vol. 288, no. 36, Sept. 2013, pp. 26179–87, doi:10.1074/jbc.M113.496968.
15. Sheinerman, Felix B., et al. "Electrostatic Aspects of Protein–Protein Interactions." *Current Opinion in Structural Biology*, vol. 10, no. 2, Apr. 2000, pp. 153–59, doi:10.1016/S0959-440X(00)00065-8.
16. Verger, Alexis, et al. "The Mediator Complex Subunit MED25 Is Targeted by the N-Terminal Transactivation Domain of the PEA3 Group Members." *Nucleic Acids Research*, vol. 41, no. 9, May 2013, pp. 4847–59, doi:10.1093/nar/gkt199.
17. Vojnic, Erika, et al. "Structure and VP16 Binding of the Mediator Med25 Activator Interaction Domain." *Nature Structural & Molecular Biology*, vol. 18, no. 4, Apr. 2011, pp. 404–09, doi:10.1038/nsmb.1997.
18. Wang, Yanming, and Charles L. Brooks III. "Electrostatic Forces Control the Negative Allosteric Regulation in a Disordered Protein Switch." *The Journal of*

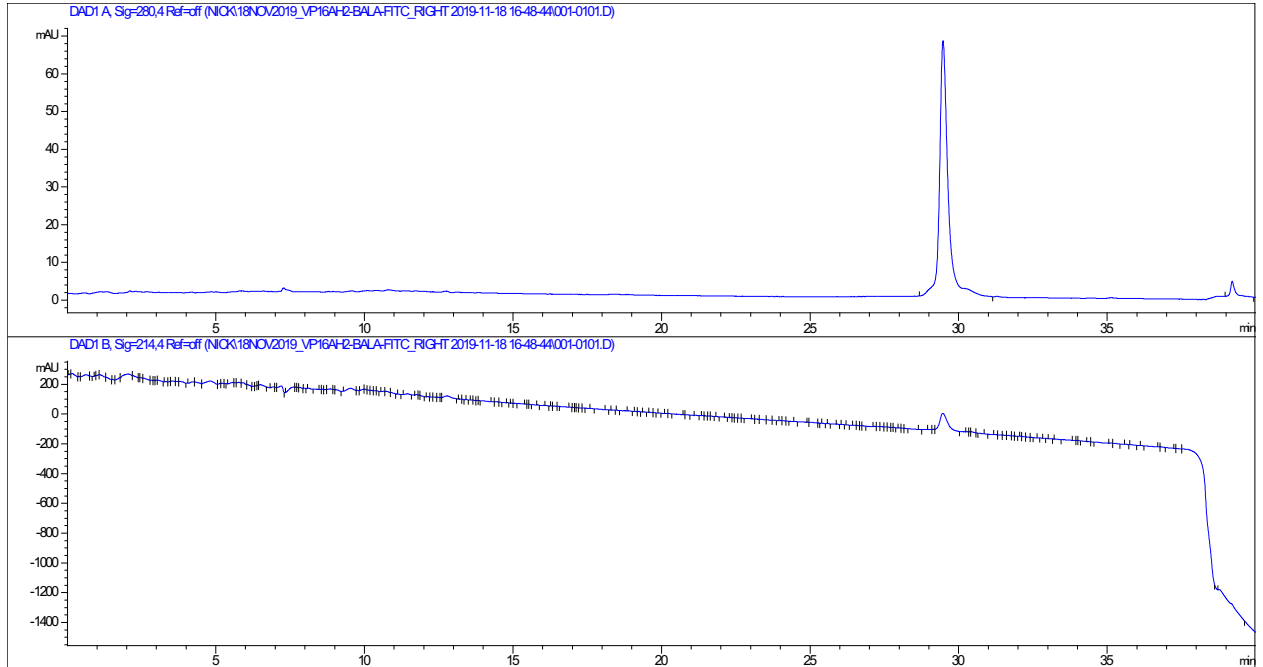
*Physical Chemistry Letters*, vol. 11, no. 3, American Chemical Society, Feb.  
2020, pp. 864–68, doi:10.1021/acs.jpcllett.9b03618.

## Appendix

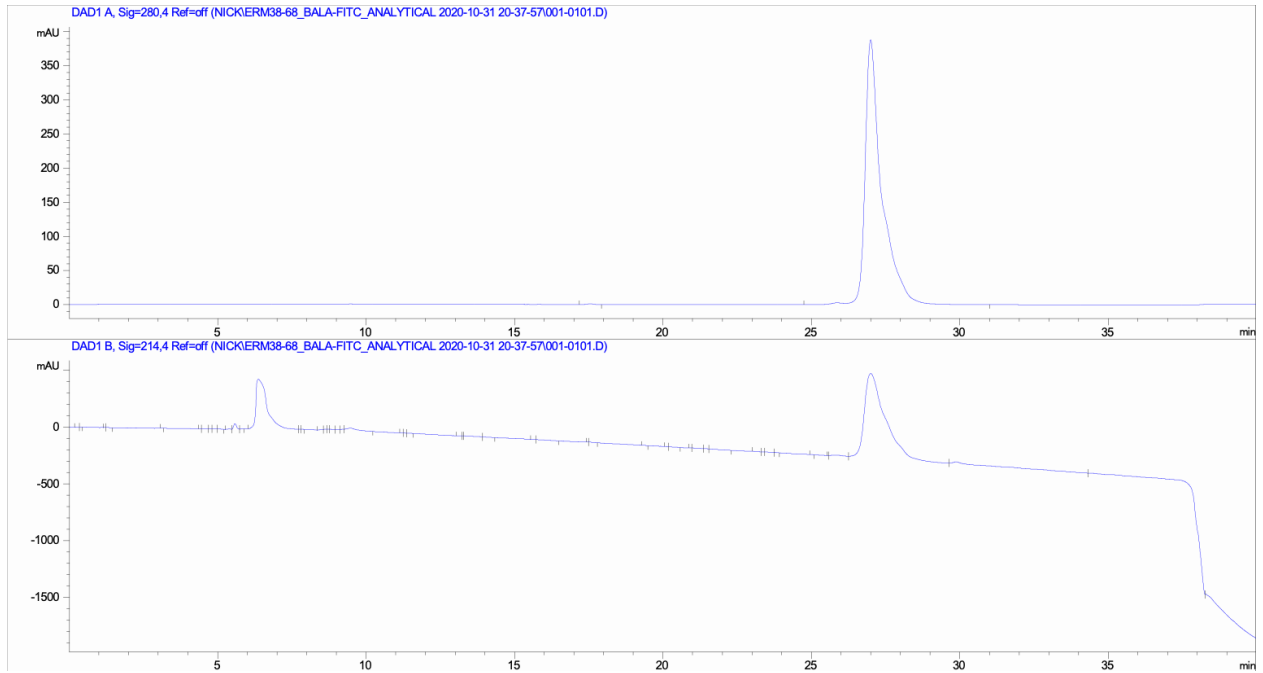
### Appendix A. Characterization of Synthesized Peptides



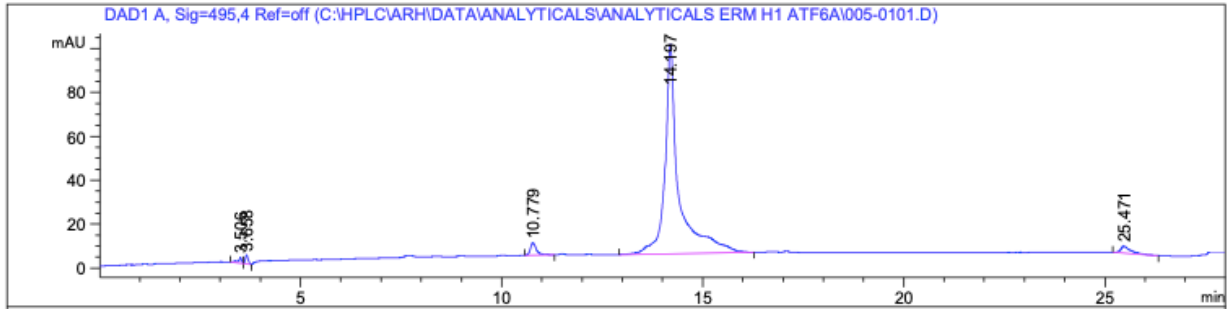
Analytical trace of **FITC-ERM<sub>38-72</sub>** monitored at wavelengths 280nm and 214nm. Samples were run in a 100mM Ammonium Acetate and Acetonitrile system.



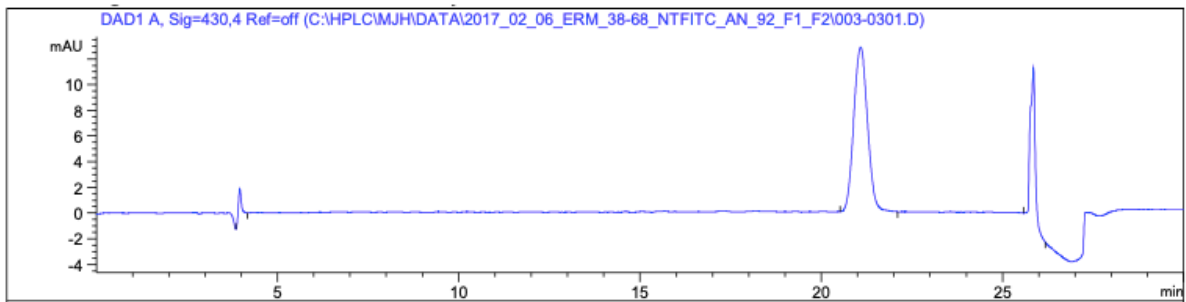
Analytical trace of **FITC-VP16 $\alpha$ H2<sub>467-488</sub>** monitored at wavelengths 280nm and 214nm. Samples were run in a 100mM Ammonium Acetate and Acetonitrile system.



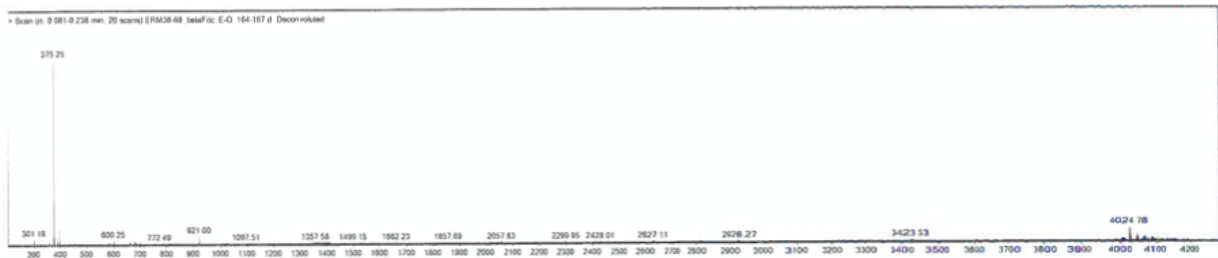
Analytical trace of **FITC-ERM<sub>38-68</sub>** monitored at wavelengths 280nm and 214nm. Samples were run in a 100mM Ammonium Acetate and Acetonitrile system.



Analytical trace of **FITC-ATF6 $\alpha$ <sub>38-64</sub>** monitored at wavelength 495nm. Samples were run in a 100mM Ammonium Acetate and Acetonitrile system.

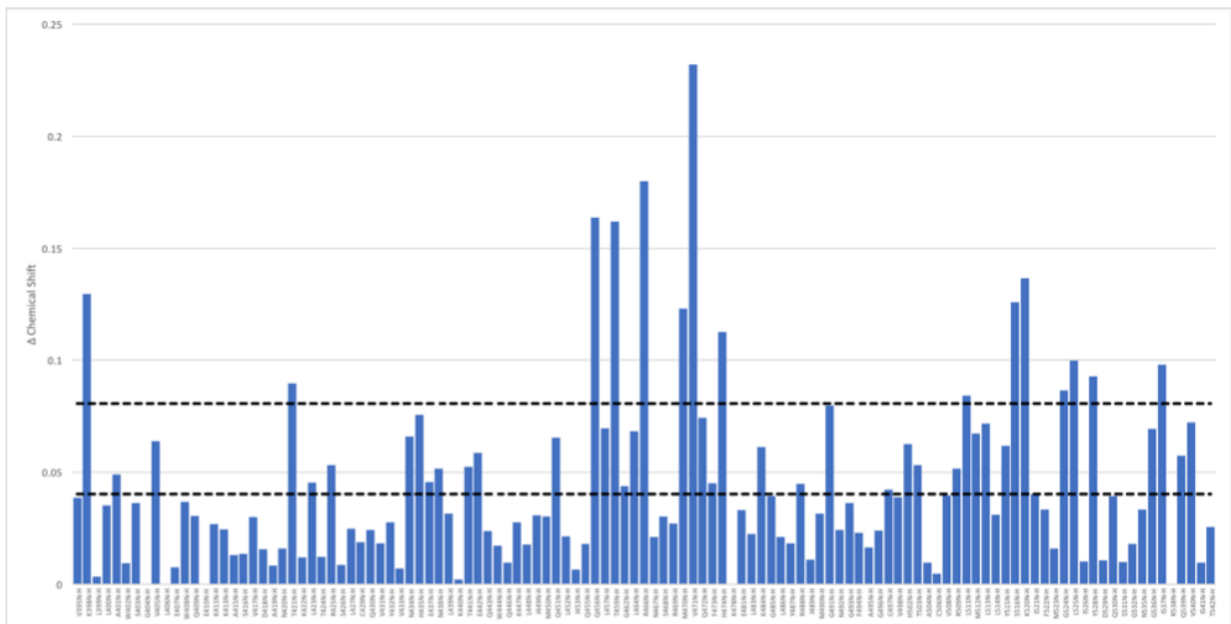


Analytical trace of **FITC-ERM<sub>38-68</sub>** monitored at wavelength 430nm. Samples were run in a 100mM Ammonium Acetate and Acetonitrile system



Mass Spectrometry spectra of **FITC-ERM<sub>38-68</sub> E-to-Q**. The peptide was quantified using Agilent's Q-tof.





CSP mapping of Med25 AcID upon titration with 1.0 eq of ATF6a(38-64). The dotted lines indicate chemical shift changes that are one (lower line) or two (upper line) standard deviations above the average chemical shift change.